Epidemic spreading on multi-layer networks with active nodes

Hu Zhang,[1,2] Lingling Cao,[1] Chuanji Fu,[1] Shiming Cai,[3] and Yachun Gao*[1]
[1)] *School of Physics, University of Electronic Science and Technology of China, Chengdu 610054, China*
[2)] *Peking University Shenzhen Graduate School, Shenzhen 518055, China*
[3)] *Big Data Research Center, University of Electronic Science and Technology of China, Chengdu 610054, China*

(*Electronic mail: gaoyachun@uestc.edu.cn)

(Dated: 18 May 2023)

Investigations on spreading dynamics based on complex networks have received widespread attention these years due to the COVID-19 epidemic, which are conducive to corresponding prevention policies. As for the COVID-19 epidemic itself, the latent time and mobile crowds are two important and inescapable factors that contribute to the significant prevalence. Focusing on these two factors, this paper systematically investigates the epidemic spreading in multiple spaces with mobile crowds. Specifically, we propose a SEIS (Susceptible-Exposed-Infected-Susceptible) model that considers the latent time based on a multi-layer network with active nodes which indicate the mobile crowds. The steady-state equations and epidemic threshold of the SEIS model are deduced and discussed. And by comprehensively discussing the key model parameters, we find that 1) due to the latent time, there is a 'cumulative effect' on the infected, leading to the 'peaks' or 'shoulders' of the curves of the infected individuals, and the system can switch among three states with the relative parameter combinations changing; 2) the minimal mobile populations can also cause the significant prevalence of the epidemic at the steady state, which is suggested by the zero-point phase change in the proportional curves of infected individuals. These results can provide a theoretical basis for formulating epidemic prevention policies.

Epidemic spreading in complex networks has received much attention in recent years, and models closer to reality have been kicked out one after another. Herein, we construct a SEIS (Susceptible-Exposed-Infected-Susceptible) model in a multi-layer network with active nodes to theoretically explore the impact of the two important factors, the latent time and mobile crowds, on the significant prevalence of the COVID-19 epidemic. Both analytical and empirical experiments are carried out to obtain the threshold of the SEIS model and key model parameters affecting the spreading dynamics in the multi-layer network with active nodes. These significant results make us deeply understand the impacts of the latent time and mobile crowds on the spreading dynamics of infectious diseases and provide a theoretical basis for formulating epidemic prevention policies.

I. INTRODUCTION

Since the outbreak of the COVID-19 epidemic in 2019, the life of human beings across the world has been greatly affected. Compared to other epidemics, such as SARS in 2003, the main characteristics of COVID-19 are its persistence in time and its large spatial transmission, which are closely related to the characteristics of the virus itself. There are three main biological factors that cause the rampant spread of COVID-19. First, it has a high transmission rate, which can be spread widely without contact through aerogel. Second, it's the latent time that can lead to the existence of 'Asymptomatic Infected Individuals', making the epidemic in the early stage of the characteristics of hidden transmission, thus not easy to inhibit its spread quickly. Third, the rapid mutation rate and the ability of COVID-19 to escape from immunity are increasing, resulting in waves of infection over time[1,2].

Another factor that influences the spread of COVID-19 is from society, mainly in the outbreak prevention and response measures[3]. Over the past three years, epidemic prevention and control policies around the world have been continuously adjusted and updated[3–5]. The overall trend of the global epidemic prevention policy now is to be 'Fully Liberalized' as the prevailing mutated strains such as XBB and BQ.1 are mainly characterized by low lethality but high transmission rate[6]. However, under such a liberalized policy, 'Universal Infection' to achieve herd immunity seems inevitable. Generally, after the liberalization policy is implemented in a country, domestic areas will experience peak infections, with only a small percentage of the population remaining totally healthy. With a very low mortality rate, implementing the liberalization policy will be beneficial in the long run for the recovery of the population and the development of the regional economy, but it will be characterized by a lack of medical resources and an increased mortality rate of seriously ill patients. Therefore, such a policy also requires a corresponding epidemic management response measure to improve the quality of life of people in an epidemic. And the development of epidemic prevention policies is supposed to be closely linked to the characteristics of the infectious disease itself, which requires accurate and in-depth research on the dynamic mechanism of the epidemic spreading.

Currently, studies on epidemic spreading in complex networks have become an effective and popular method[7–10]. The 'Node-Edge' network is closely related to the real-life social relationships between individuals, which provides a theoretical framework for epidemic spreading. Since the traditional

SI, SIS, and SIR models were proposed, the epidemic spreading models based on complex networks have become more and more abundant and realistic[11,12]. ***Later, due to the latent time of some infectious diseases, scholars have introduced the Exposed State E in the process and have constructed the classical SEIR model to simulate the real disease transmission process, which has been also widely used in the study of the epidemic of COVID-19 these days***[13–15]**.**

However, the process of disease transmission depends not only on the intrinsic biological properties of the virus, but also on social factors (e.g., epidemic prevention policies, individual alertness, different geographic spaces, etc.). The intricacies of social factors make it difficult to understand the intrinsic mechanism of disease transmission accurately, and also make the process of disease transmission characterized by 'peaks', periodic outbreaks and other phenomena[16]**. Therefore, more studies have taken social factors into consideration in depth these days.*** An increasing number of studies focus on the introduction of society parameters, such as the inclusion of panic psychology[17] and social safety distance[18] in the models, ***and some try to optimize the propagation model according to the real situation, such as setting new states in the propagation process***[19]***, exploring the topology mechanism based on network structure***[20]***, etc.*** In addition, immunization strategies[21,22] and resource allocation[23,24] are also important elements in the study of epidemic spreading. When an epidemic occurs, the development of immunization strategies that can contain the spread of the disease quickly, and the allocation of limited individuals or social resources are hot spots in the study of transmission dynamics of complex networks. In addition, after the introduction of multi-layer networks[25–28], the study of epidemic spreading has been enriched. For example, works on 'Information-Disease Coupling Networks'[29,30] and 'Socio-Biological Transmission Systems'[31,32] based on multi-layer networks have achieved a lot of results and laid the theoretical foundation for the policy guidance of epidemic prevention. However, most of them are still devoted to exploring the comprehensive influence of different functional spaces in multi-layer networks on the spreading process, and relatively few works have been done on the disease transmission behaviour among different geographical spaces (e.g., different cities, different countries) based on multi-layer networks. However, the 'layers' in multi-layer networks are a good abstraction of different geographic spaces, which can also be a major concern for researchers.

At the same time, the diversity of social activities and the complexity of the network structure make the study of epidemic spreading still have much room for development. First, most of the current works on epidemic spreading dynamics in complex networks focus on the topology of the network, while the influence of the spreading dynamics itself on the transmission process, such as its characteristics and state transition mechanisms, is still neglected and needs to be further explored. Second, most of the multi-layer networks focus on each functional space, but from COVID-19, the movement of some people among geographic spaces is one of the key factors causing the epidemic outbreak in the whole region, so it is urgent to study the multi-layer networks in combination with geographic spaces[33]. In addition, the social factors affecting the transmission process are too diverse to be considered comprehensively, and the selection of important social factors for proper quantification is also a great challenge for epidemic spreading in complex networks, so it's hard to keep a balance between parameter selection and model simplification. To address these issues, this paper models the epidemic spreading in a multi-layer network by introducing 'active nodes'[32,34] that simulate the mobile crowds in each patch. In addition, to focus on the impact of the incubation period of (infectious) diseases, the exposed state E is coupled into SIS model based on Markov chain[34,35]. Totally, a SEIS (Susceptible-Exposed-Infected-Susceptible) model based on the multi-layer network with active nodes is established here to explore the dynamics mechanism of the diseases with the incubation among multiple spaces due to the mobile crowds.

II. THE MODEL

The model contains two main dimensions: the vertical random walk of active nodes and the horizontal disease transmission. As for the vertical dimension, we use a layer in the multi-layer network to represent the smallest unit of each geographic space (e.g., a city). In each layer, there are a certain number of static nodes and edges, constituting the static network structure of the layer. The inter-layer connections are then established through active nodes, which can be bound randomly across different layers[32,34]. From the perspective of discrete time, the active nodes can randomly jump from one layer to another at each time unit, thus making the whole network time-varying. As for the horizontal dimension, we add the exposed state E to the SIS model (i.e., SEIS model) to explore the spread of diseases with the incubation in the time-varying multi-layer network.

An example of a three-layer network model is provided here to vividly describe the random-walk process of active nodes, as shown in Fig. 1. The network contains a total of six active nodes (marked in orange), which at the initial moment (Fig. 1, left) are equally distributed among the layers, numbered 1 to 6. There are also several static nodes (marked in blue) in each layer of the network. The fixed edges between each active node and static node in each layer are determined first, and only when an active node wanders to the right layer, these edges are activated, thus changing the network structure in that layer. After a time interval Δt, the active nodes wander randomly on the three-layer network, where the active nodes No.2 and No.6 wander to the second layer, and the remaining active nodes remain unchanged at the original layer (Fig. 1, right). For the sake of discussion, it is assumed that active nodes are not memorable, i.e., when an active node hops to a layer, the wandering result at the next moment is only related to the layer it is currently on, and not to the layer it was at before.

Based on this multi-layer network, a 'seed infected node' (I state) is set at the initial moment, and the nodes of the whole network evolve in the SEIS mode. Due to the recovery rate, the system can reach a steady state after a certain period

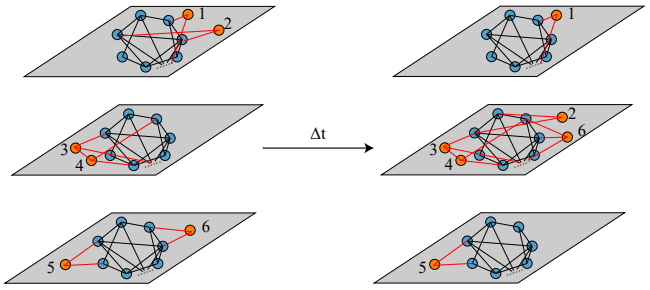

FIG. 1. An example of random-walk process for active nodes. ***The nodes marked orange are active, while the blue ones are static. The left side shows the position state of each node at the initial moment, and the right side shows the position state of each node after Δt. In this example, active node No.2 jumps from the topmost level to the middle level, active node No.6 jumps from the bottom level to the middle level, and the remaining nodes stay unchanged.***

of time, and the transition between the nodes reaches a dynamic equilibrium. The random wandering of active nodes in the model is carried out vertically between layers, while the spread of a disease is carried out horizontally across layers. The connection between the vertical and horizontal behaviour is established through the active nodes, i.e., an active node that wanders vertically may carry the disease from one layer to another, which in turn leads to horizontal disease transmission behaviour in that layer. Therefore, due to the different dynamical behaviour of the two dimensions, we will discuss them separately as follows.

A. The Vertical Random-Walk Process for Active Nodes

Let the layers' number of the multi-layer network be D. For simplicity, each layer can be represented by an unweighted and undirected graph. For the layer $d(1 \le d \le D, d \in N^*)$, the corresponding graph is denoted as $G^d = \left(V^d, E^d\right)$, where V^d represents the set of nodes at layer d and E^d represents the edges set. Thus we have $\mathscr{G} = (\mathscr{V}, \mathscr{E}), \mathscr{V} = \bigcup_{d=1}^{D} V^d, \mathscr{E} = \bigcup_{d=1}^{D} E^d$, where $\mathscr{G}$ denotes the whole multi-layer network, while $\mathscr{V}$ and $\mathscr{E}$ represent the set of nodes and edges of the whole network, respectively. Let each layer of the network contain m static nodes, while the multi-layer network contains a total of n active nodes that can jump randomly across the layers, then each layer has at most $(m+n)$ nodes. Then we set the adjacent matrix of the multi-layer network containing active nodes $\boldsymbol{A}_{Mul}$ as[26,27]

$$\boldsymbol{A}_{Mul} = \begin{pmatrix} \boldsymbol{A}_{St}^{1} & 0 & \cdots & 0 & \boldsymbol{C}^{1n} \\ \boldsymbol{C}^{21} & \boldsymbol{A}_{St}^{2} & \cdots & 0 & \boldsymbol{C}^{2n} \\ \vdots & \vdots & \ddots & \vdots & \vdots \\ 0 & 0 & \cdots & \boldsymbol{A}_{St}^{D} & \boldsymbol{C}^{Dn} \\ \boldsymbol{C}^{n1} & \boldsymbol{C}^{n2} & \cdots & \boldsymbol{C}^{nD} & \boldsymbol{A}_{Act} \end{pmatrix}, \tag{1}$$

where $\boldsymbol{C}^{nd} = \left(\boldsymbol{C}^{dn}\right)^T$ are both time-varying matrices, which reflects the concatenated edge information of n active nodes with m static nodes at each level, with a dimension of $n \times m$ for $\boldsymbol{C}^{nd}$. $\boldsymbol{A}_{St}^{d}$ represents the relationship between the edges of the static nodes in d-th layer, i.e., the static network in each layer, which does not change with time. Since there are m static nodes in each layer, the dimension of $\boldsymbol{A}_{St}^{d}$ is $m \times m$. In addition, $\boldsymbol{A}_{Act}$ represents the edge relationship between n active nodes with dimension $n \times n$. We consider that there is no correlation among active nodes, thus we have $\boldsymbol{A}_{Act} = \boldsymbol{0}$.

So far, the structure of the whole multi-layer network is stored through the adjacency matrix $\boldsymbol{A}_{Mul}$. But the transmission process is based on each layer, so for the convenience of subsequent discussion, it is necessary to focus on the network structure of each layer, which is time-varying due to the introduction of active nodes. To simplify the model, it's useful to consider each layer as a combination of a static network and a time-varying network with active nodes, so the adjacency matrix $\boldsymbol{A}^d$ of each layer network is set as

$$\boldsymbol{A}^d = (a_{ij})_{(m+n)\times(m+n)} = \begin{pmatrix} \boldsymbol{A}_{St}^{d} & \boldsymbol{A}_{Var}^{d} \\ \left(\boldsymbol{A}_{Var}^{d}\right)^T & \boldsymbol{0} \end{pmatrix}, \tag{2}$$

where $\boldsymbol{A}_{St}^{d}$ still stores the static network structure of each layer, and $\boldsymbol{A}_{Var}^{d}$ represents the dynamic network structure formed by the edges between n active nodes and m static nodes in the layer d network, which is time-varying with dimension $m \times n$. If the active node i is not in this layer, the matrix elements of both row i and column i in $\boldsymbol{A}_{Var}^{d}$ are set as 0.

Through the discussion above, the total adjacency matrix and the adjacency matrix of each layer are established separately, with the network structure synchronously determined. For any active node $i-Act$, the following record is made: (1) An inter-layer transfer matrix $\boldsymbol{L}_{i-Act}(t) \mid= \left[l_{jk}(t)\right]_{D\times D}$ is set to record the probability of active node $i-Act$ jumping from the j_{th} layer to the k_{th} layer through the element l_{jk}. (2) A layer state vector $\boldsymbol{V}_{i-Act}(t) = \left[v_i(t)\right]_{1\times D}$ is set to determine whether the active node $i-Act$ is in layer d. $v_i(t)$ is a 0-1 variable that indicates if the active node $i-Act$ is right in the layer only when $v_i(t) = 1$ and $v_i(t)$ at any moment only has one element of 1. (3) A layer probability vector $\boldsymbol{W}_{i-Act}(t) = \left[w_i(t)\right]_{1\times D}$ is set to record the probability that node $i-Act$ is in each layer at the moment t. Thus the sum of all elements in $\boldsymbol{W}_{i-Act}(t)$ is 1. Then we can obtain[34]

$$\boldsymbol{W}_{i-Act}(t+1) = \boldsymbol{V}_{i-Act}(t)\boldsymbol{L}_{i-Act}(t). \tag{3}$$

After we get the layer probability vector of time $t+1$: $\boldsymbol{W}_{i-Act}(t+1)$, we can use a randomization process of the probabilities to determine the right layer that active node i located in. After a long time, the random walk of active nodes will reach a steady state, i.e., the probability of being in each layer is constant. So we have $\boldsymbol{W}_{i-Act}(t) = \boldsymbol{W}_{i-Act}(t) = \boldsymbol{\pi}_{i-Act}$ at the steady state, where the element $\boldsymbol{\pi}_{i-Act}$ represents the probability that active node i is in each layer at steady state.

B. The Horizontal Disease Transmission

For any node i on the multi-layer network (both static and active nodes), there are two records being made: (1) A 1×3

node state vector $\boldsymbol{s}_i(t) = \left[s_i^X(t)\right]$ is set to record the state of a node during the disease transmission process, where $X = S, E, I$ when node i is in S, E, I state, respectively. In this paper, the element states in $\boldsymbol{s}_i(t)$ are in the order of S, E, and I, i.e., $\boldsymbol{s}_i(t) = \left[s_i{}^S(t), s_i^E(t), s_i{}^I(t)\right]$. When node i is in state X, then $s_i^X(t) = 1$, otherwise 0. At any moment for each $\boldsymbol{s}_i(t)$ there is only one element that is 1. (2) A node probability vector $\boldsymbol{p}_i(t)$ is set to denote the probability that node i is in the X state at the moment t and $\boldsymbol{p}_i(t) = \left[p_i^X(t)\right] = \left[p_i^S(t), p_i^E(t), p_i^I(t)\right]$.

In our SEIS model, the specific meaning of each state and the mechanism of transition between states are as follows: (1) The state S (Susceptible), is to simulate the healthy individuals. Any node in state S can be infected by neighbour nodes in state I with probability β, and can also be infected by neighbours in state E with probability β^E. If the node in state S is successfully infected, it is transformed into state E; (2) ***The state E (Exposed), is to simulate the asymptomatic infected individuals who can infect others.*** Any node in state E can be transformed to state I with probability α, and α is called the 'Expose Rate' in this paper; (3) The state I (Infected), is to simulate those who have developed symptoms in the process of the disease spreading. Any node in state I state any node can be restored to the S state with probability γ, which is called the 'Recovery Rate' in this paper. Besides, inspired by available literature[17], α is usually got from the average latency days T_E: $\alpha = 1/T_E$. Similarly, γ can be obtained through $\gamma = 1/T_I$, where T_I denotes the average recovery days.

Then we use the discrete Markov chain approach to establish the propagation equations. Considering the network structure, let $q_i(t)$ denote the probability that any node i is infected by receiving information from all neighbour nodes at the moment t, according to the different descriptions of $q_i(t)$, we have two kinds of representations for the horizontal disease transmission[32,34].

1. Stochastic Representation

Stochastic representation of disease spreading is applied for numerical simulations. For each layer, the minimum number of nodes at any moment is m and the maximum number of nodes is $m+n$. To incorporate all cases, an all-nodes state matrix $\boldsymbol{S}^d(t) = \left[\boldsymbol{s}_i(t)^{\boldsymbol{T}}\right]$ is set to store the states of all nodes in d_{th} layer, with a dimension of $3 \times (m+n)$. We have $\boldsymbol{S}^d(t) = \left[\boldsymbol{s}_1(t)^{\boldsymbol{T}}, \boldsymbol{s}_2(t)^{\boldsymbol{T}}, \ldots\ldots, \boldsymbol{s}_m(t)^{\boldsymbol{T}}, \ldots\ldots, \boldsymbol{s}_{m+n}(t)^{\boldsymbol{T}}\right]$, where the first m column vectors are the node state vectors of the static nodes and the last n column vectors are the node state vectors of the active nodes. Then let $\boldsymbol{G}^d(t) = \boldsymbol{S}^d(t)\boldsymbol{A}^d(t)$, so $\boldsymbol{G}^d(t)$ is used to store the number of neighbour nodes in each state for all nodes in each layer. Specifically, for the storage model of $\boldsymbol{s}_i(t) = \left[s_i^S(t), s_i^E(t), s_i^I(t)\right]$, the first row of $\boldsymbol{G}^d(t)$ represents the number of S-state nodes adjacent to node i in the d_{th} layer and is denoted as $g_i^S(t)$, the second row represents the number of E-state nodes adjacent to each node and is denoted as $g_i^E(t)$, while the third row represents the number of I-state nodes adjacent to node i and is denoted as $g_i^I(t)$. ***So the probability that an S-state node is not infected by any neighbor E-state node at time t is $(1-\beta^E)^{g_i^E(t)}$, while the probability that an S-state node is not infected by any neighbor I-state node at time t is $(1-\beta)^{g_i^I(t)}$.*** Then we have

$$q_i^E(t) = 1 - \left(1-\beta^E\right)^{g_i^E(t)}, \tag{4a}$$

$$q_i^I(t) = 1 - (1-\beta)^{g_i^I(t)}, \tag{4b}$$

where $q_i^E(t)$ denotes the probability that node i is infected by E-state neighbors at moment t, and $q_i^I(t)$ denotes the probability that node i is infected by I-state neighbors at moment t. Hence, the the probability $q_i(t)$ of node i unfortunately becoming infected is

$$q_i(t) = q_i^E(t) \cup q_i^I(t) = q_i^E(t) + q_i^I(t) - q_i^E(t)q_i^I(t). \tag{5}$$

Eq.(5) is because the propagation process between each two individuals is assumed to be independent of each other. In turn, the randomized difference equation for the disease transmission process can be obtained as

$$p_i^S(t+1) = s_i^S(t)\left(1-q_i(t)\right) + \gamma s_i^I(t)\left(1-q_i(t)\right), \tag{6a}$$

$$p_i^E(t+1) = (1-\alpha)s_i^E(t) + s_i^S(t)q_i(t) + \gamma s_i^I(t)q_i(t), \tag{6b}$$

$$p_i^I(t+1) = \alpha s_i^E(t) + (1-\gamma)s_i^I(t). \tag{6c}$$

Each item of the right side in the equations represent one of the sources of the left side. Specifically, there are two contributions to the probability of being S state at moment $t+1$ for a node, as shown in Eq.(6a). The first term on the right-hand side represents the probability that a S-state node i is not infected at moment t, while the second term represents the probability that an I-state node i recovers to a S-state and meanwhile is not re-infected. Eq.(6b) gives the probability a node is in E state, in which the first term on the right-hand side stands for an E-state node is not changing to an I-state, and the second term comes from a S-state node being infected and converting to E state, while the third term comes from the recovered I-state node suffering from re-infection to become an E-state. Eq.(6c) gives the probability of being I state. the first term on the right represents that an E-state node become an I-state node as a probability of α, and the second term gives the probability of an I-state node remaining as an I-state.

Besides, Eq.(4) can be also marked as

$$q_i^E(t) = 1 - \prod_{j \in Nei(i)} \left[1 - \beta^E s_j^E(t) v_j^d(t) v_i^d(t)\right], \tag{7a}$$

$$q_i^I(t) = 1 - \prod_{j \in Nei(i)} \left[1 - \beta s_j^I(t) v_j^d(t) v_i^d(t)\right], \tag{7b}$$

where $Nei(i)$ represents the set of neighbor nodes of i. And $s_j^E(t)$,$s_j^I(t)$ are the elements in the Node State Matrix Vector $\boldsymbol{s}_j(t)$, which are 0-1 variables; $v_j^d(t)$,$v_i^d(t)$ are used to determine whether node j, i is in the d_{th} layer at time t. Their values are 1 if they are in the d_{th} layer, or 0 otherwise, which is a generalization of the elements in the layer state vector $\boldsymbol{V}_{i-Act}$, so that its physical meaning also applies to static nodes.

2. Deterministic Representation

The above stochastic representation is applied for theoretical analysis. Next, we replace the 0-1 variable $s_i^X(t)$ by the Markov probability $p_i^X(t)$, i.e., characterize the states in the form of probabilities. Then, $q_i^E(t)$, $q_i^I(t)$ can be calculated as follows:

$$q_i^E(t) = 1 - \prod_{j \in Nei(i)} \left[1 - \beta^E p_j^E(t) w_j^d(t) w_i^d(t)\right], \tag{8a}$$

$$q_i^I(t) = 1 - \prod_{j \in Nei(i)} \left[1 - \beta p_j^I(t) w_j^d(t) w_i^d(t)\right]. \tag{8b}$$

where $w_j^d(t)$, $w_i^d(t)$ are the elements in the layer probability vector $\boldsymbol{W}_i(t)$, denoting the probability that nodes j and i are at the d_{th} layer at the moment t, respectively, and the values of which are 1 or 0 for static nodes while taking the range [0,1] for active nodes. In view of this, the probability of node i being infected by neighbour nodes at moment t can be found by finding the merge set, just as Eq.(5) shows.

Under this circumstance the propagation equation can be obtained as

$$p_i^S(t+1) = p_i^S(t)\left(1 - q_i(t)\right) + \gamma p_i^I(t)\left(1 - q_i(t)\right), \tag{9a}$$

$$p_i^E(t+1) = (1-\alpha) p_i^E(t) + p_i^S(t) q_i(t) + \gamma p_i^I(t) q_i(t), \tag{9b}$$

$$p_i^I(t+1) = \alpha p_i^E(t) + (1-\gamma) p_i^I(t). \tag{9c}$$

Strictly speaking, the items on the right side of the three equations above should be taken as a merged set, but due to the independence of each sense, the small amount can be ignored after the expansion of the addition theorem of independent events. Besides, we have $p_i^S + p_i^E + p_i^I = 1$ at any time.

When it comes to the steady state, we have $p_i^X(t+1) = p_i^X(t)$, thus two important steady-state (denoted with an asterisk) propagation equations can be obtained from Eq.(9) as

$$\frac{\left(p_i^E\right)^*}{\left(p_i^I\right)^*} = \frac{\gamma}{\alpha}, \quad \forall i, \tag{10}$$

and

$$\left(p_i^I\right)^* \left[\gamma + \left(1 - \gamma + \frac{\gamma}{\alpha}\right) q_i^*\right] - q_i^* = 0, \quad \forall i. \tag{11}$$

Since Eqs.(10) and (11) holds for any node, and according to the statistical significance, they also represent the proportion of nodes in each state among the whole network at the steady state. That is, $(p_i^I)^*$, $(p_i^E)^*$ give the proportion of nodes in E and I states, respectively, and q_i^* indicates the proportion of nodes be infected. Therefore, it can be concluded that the ratio of I-state nodes to E-state nodes is constant at steady state and is equal to the ratio of recovery rate to expose rate.

Particularly, let $\alpha \to \infty$. At this point, α is no longer meaningful as a probability, but we've mentioned that $\alpha = 1/T_E$ (T_E represents the average latency days), so $\alpha \to \infty$ represents $T_E \to 0$, i.e., there is no longer incubation for the disease. So the model degenerates to the SIS model, Eq.(11) becomes

$$\left(p_i^I\right)^* \left[\gamma + (1-\gamma) q_i^*\right] - q_i^* = 0, \quad \forall i, \tag{12}$$

which is consistent with the steady-state equation form of the SIS model from Li et al.'s achievement[32], indicating that our model can extra depict the influence of the latent time.

Obviously, $\boldsymbol{P} = \boldsymbol{0}$, which denotes $\left(p_i^I\right)^* = 0$ for all the nodes, is the solution to Eq.(11), and thus $\left(p_i^E\right)^* = 0$ according to Eq.(10), representing no outbreak of the disease. In addition, according to the characteristics of nonlinear dynamical systems, besides $\boldsymbol{P} = \boldsymbol{0}$, there are non-trivial solutions satisfying Eq.(11), in which the system finally reaches the dynamic equilibrium: the ratio of the three states fluctuates steadily around a certain fixed value, and the point of $\boldsymbol{P}$ is the 'Epidemic Equilibrium Point' of the system. After the parameters of the system are determined, it evolves toward these two solutions, and the evolution time depends on the internal characteristics of the system. The epidemic equilibrium points can be calculated by numerical simulation through Eq.(11), which can be also divided into 'General-Epidemic Equilibrium State' and 'Full-Domain Outbreak State' according to the proportion that get infected. If there is a super high contagion coverage in the steady state, then the system goes into the Full-Domain Outbreak State, otherwise, in the General-Epidemic Equilibrium State. To measure the scale of infection of the whole network, the ordinal parameter $\left(\rho^X\right)^*$ is introduced here as

$$\left(\rho^X\right)^* = \frac{1}{N} \sum_{i=1}^{N} \left(p_i^X\right)^*, \tag{13}$$

representing the density of states of the nodes $\left(\rho^X\right)^*$ at steady state, where N denotes the total number of nodes in the multi-layer network. Besides, it is usually concerned with how many nodes are in unhealthy states at steady state, i.e., the sum of E and I states, and incorporating both E and I states into a new state: the V state (V is the first letter for Virus-Carrier), the proportion of V-state nodes at steady state is simply denoted as ρ^*, so

$$\rho^* = \left(\rho^E\right)^* + \left(\rho^I\right)^* = 1 - \left(\rho^S\right)^*, \tag{14}$$

which will be used to discuss the results later.

Since there are a large number of symbols, we present the names and definitions of the main symbols in Appendix A.

C. The Epidemic Threshold

The epidemic threshold of an infectious disease is an important parameter to measure the ability of a disease to spread on a large scale[9–11], which can be found by discussing the asymptotic stability of the point $\boldsymbol{P} = \boldsymbol{0}$[9]. Given that in reality it is concerned about how many individuals getting infected, rather than individuals with symptoms, we analyze the threshold with the V-state mentioned above. Thus, analogous to the above discussion, the deterministic difference equation for the V-state can be listed as follows.

$$p_i(t+1) = \left[1 - p_i(t)\right] q_i(t) + p_i(t)\left[(1-\gamma) + \gamma q_i(t)\right], \tag{15}$$

where we use $p_i(t)$ to uniformly represent the probability that any node (not just i) is in state V at moment t. And according

to Deepayan et al.'s method[9], we can draw a conclusion as shown in Eq.(16),

$$\tau_c = \left(1+\frac{\gamma}{\alpha}\right)\frac{1}{\lambda_{\max,\boldsymbol{B}}}, \tag{16}$$

Here, $\lambda_{\max,\boldsymbol{B}}$ is the maximum eigenvalue of the matrix $\mathbf{B}$ related to the adjacency matrix of the multiplex network as well as the layer state of active nodes, which is introduced in detail in Appendix B.

As shown in Eq.(16), the epidemic threshold in the model is mainly determined by two factors. One is the ratio of the expose rate α to the recovery rate γ, which reflects the characteristics of the propagation process. And the other is the parameter $\lambda_{\max,\boldsymbol{B}}$, which is related to the network topology structure, also implying the influence of active nodes. The random wandering of active nodes makes the network time-varying, but active nodes tend to be few in reality, and the general structure of the whole multi-layer network remains unchanged, so the epidemic threshold can be calculated by averaging Eq.(16) over several experiments.

III. RESULTS AND DISCUSSIONS

In this section, we focus on the intrinsic effects of the parameters in the model on the propagation process, with the number of active nodes, the expose rate α, the recovery rate γ, and the virus transmission rate β, β^E explored in depth. In the numerical simulation, the number of layers of the multi-layer network is set to $d = 5$. To better simulate the power-law distribution obeyed by real-life social networks, each layer is set to be a BA scale-free network. Meanwhile, the number of static nodes in each layer is $m = 10000$. We carry out 100-time simulations to eliminate fluctuations. For the convenience of subsequent discussion, $\delta = \frac{n}{m}$ is defined as the relative proportion of active nodes. The results are detailed below.

1. The Relative Proportion of Active Nodes

The Relative Proportion of Active Nodes is an important parameter in our model, which can be roughly obtained from the mobile phone geolocation data[36]. In the literature[36], the data of individuals' movements of Wuhan during 1-24 January, 2020 is collected, and this is the time before the lockdown policy of Wuhan. Thus we can obtain its relative proportion of active nodes of about 0.043, while it is during the Chinese Spring Festival when the mobile crowds is more significant, so we set the maximum relative proportion to 0.1 in our experiment. Then, five different values of $\delta(\delta = 0, 0.0001, 0.001, 0.01, 0.1)$ are simulated with other parameters set as $\beta = 0.01, \beta_E = 0.12, T_E = 7, T_I = 21$, ***where*** $\delta = 0$ ***can simulate the lockdown policy,*** $\delta = 0.0001$ ***simulates the light-lockdown policy(i.e, very few individuals can move),*** $\delta = 0.001$ ***simulates the normal-state life of individuals,*** $\delta = 0.01$ ***simulates the holidays, and*** $\delta = 0.1$ ***simulates the extreme cases.*** Besides, in order to satisfy the practical cases, the average latency days T_E and the average recovery days T_I are used to replace α, γ for intuitively better understanding. The results are shown in Fig. 2. It can be seen that with the increase of δ, the steady-state proportions of I-state nodes, E-state nodes and V-state nodes also increase simultaneously, and for the E-state curves, there is some 'peaks' (Fig. 2(b)), the larger the δ, the higher and narrower the peak, which is related to the rapid accumulation of asymptomatic infected individuals. Also, V-state curve appears the phenomenon of 'shoulders' with the increase of δ to 0.1 (Fig. 2(c)).

The phenomenon of 'shoulders' and 'peaks' is consistent with the initial outbreak of some infectious diseases with incubation periods (e.g., the COVID-19 epidemics), and some scholars have explored the mechanism of the emergence of 'shoulders' and 'peaks'[17], but we believe that one important reason is the introduction of the latent period resulting in asymptomatic infected individuals, which is called the 'cumulative effect' here. The relative proportion of active nodes can induce the 'cumulative effect', as long as δ reaches a certain value, the 'cumulative effect' works: when the disease initially spreads, the infection process (an S-state node getting infected to the E-state) of the whole system proceeds very fast due to the high number of S-states in the system, and on the other hand, the speed of the exposing process, in which a node evolves from E state to I state, is relatively low, resulting in the accumulation of the number of E states. After a period of time, with the accumulation of the number of E-state nodes and the decrease of the number of S-state nodes, the speed of the exposing process gradually increases, while the infection process slows down, and eventually, the number of E-state individuals begins to fall back to the steady state. The same analysis can be used to explain the 'shoulders' appearance of the V-state curves, where the shift from 'peaks' to 'shoulders' is because the V-state nodes contain the I-state nodes, which weakens the accumulation process of the number of nodes in the E state.

In addition, we can clearly see from the figure that when $\delta = 0$***, the proportions of I-state, E-state and V-state nodes in the steady state is much lower than other cases, and the corresponding curves do not show "shoulders" or "peaks". This is because when*** $\delta = 0$***, there is no active nodes in the system, so the inter-layer connection of each layer is broken, thus the virus can only spread in that layer and cannot form a large-scale outbreak in the whole area. This is also consistent with reality and shows that when a new infectious disease emerges, a timely lockdown policy can block the spread and can inhibit the formation of infection peaks. And when a light-lockdown policy is implemented (*$\delta = 0.0001$***), the final proportions of** V***-state nodes caused by even few active nodes is already larger than 0.6, which indicates that a small number of active nodes can cause a large amount of spread, and this conclusion will be verified in the following simulation experiments. We also found that in the four cases with*** $\delta \neq 0$***, the proportion of** E***-state nodes in steady state does not differ much, and the proportion of** I***-state nodes increases slowly, indicating that although the introduction of the latent time causes cumulative effects, it does not affect***

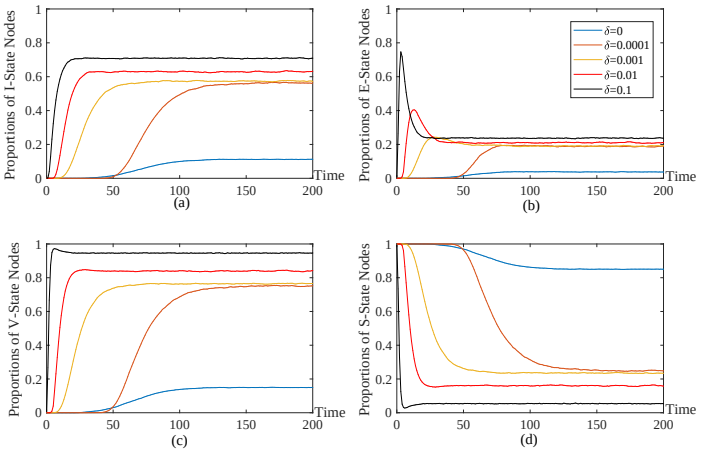

FIG. 2. The evolution of the proportions of each state node with time for different δ (Figures (a), (b), (c) and (d) show the proportions of I-state node, E-state node, V-state node and S-state node in order, and the remaining parameters are set to $\beta = 0.1$, $\beta^E = 0.12$, $T_E = 7$ and $T_I = 21$.)

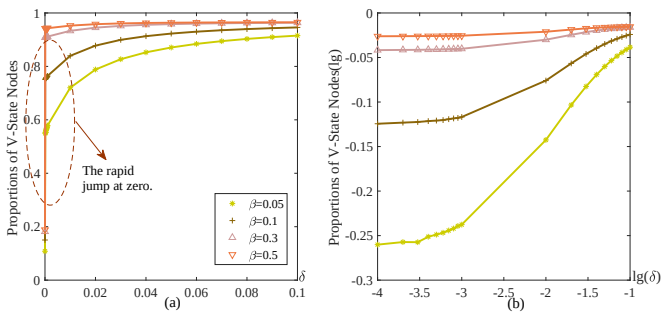

FIG. 3. The proportions of V-state nodes at steady state ρ^* as a function of δ, the proportion of active nodes. (a) is the direct result, and (b) is the result in double logarithmic coordinates for a clear observation. Other parameters: $\beta^E = 1.2\beta, T_E = 7, T_I = 21$.

the transition of nodes from transimission states, and most of the infected nodes will eventually stay in I-state.

Next, in order to explore the effect of δ (the relative proportion of active nodes) on the propagation more clearly, the proportion of V-state nodes at steady state ρ^* is selected as the sequential parameter, changing with δ under four groups (β, β^E), as shown in Fig. 3, where $\beta = 0.05, 0.1, 0, 3, 0.5, \beta^E = 1.2\beta, T_E = 7, T_I = 21$, and the number of multi-layer network layers and network structure are consistent with previous experiments.

As can be seen in Fig. 3(a), the influence of the relative ratio of active nodes on the disease infection process is reflected in the rapid jump at zero: the phase change of ρ^* occurs at $\delta = 0$ conformably for different β and then slowly stabilizes, which means that there is no threshold for δ. To see this fast jump more visually, a double-log curve is provided as shown in Fig. 3(b). Further, it is noted that the value of ρ^* even tends to steady state rapidly when $\delta = 0.0001$ (i.e., there is only one active node in the network), indicating that when the homeostasis of the system is the epidemic equilibrium state, the disease can develop as long as one node can flow. Besides, a larger β is more conducive to the spread of disease, and, together with δ can induce the infection process with a larger zero-point phase transition span. Thus the introduction of active nodes further facilitates the spread of the disease, but it cannot change the steady-state value. So what matters in the steady-state is whether there is the movement of crowds, not how much movement. However, due to social development factors, it's not advisable to prohibit people from moving, so how to manage mobile crowds is more important than restricting people from traveling during epidemics. ***Once the epidemic has reached a steady state, it's more recommended to focus on how to provide effective treatment and care for patients and optimize epidemic prevention measures to stop the spread of the disease while also ensuring that the lives of others are not too affected. So focusing on the COVID-19 epidemic under the current stage where the steady state has reached, it's advisable that many areas have adopted the liberal policy of not restricting the movement of people on a large scale everywhere.***

2. The Combined Effects of The Expose Rate and Recovery Rate

Inspired by Eq.(16), the combined effects of expose rate α and recovery rate γ on the disease transmission process are explored below. The experiments are carried out for (α, γ) traversed between [0,1]. For continuity, we use expose rate and recovery rate here, but it is intuitively meaningful of their inverse, the average latency days and the average recovery days, respectively. Here we provide an example with other parameters being set to $\beta = 0.01, \beta^E = 0.12, \delta = 0.001$, still taking the steady-state V-state nodes ratio ρ^* as the order parameter, and obtaining $\rho^* - (\alpha, \gamma)$ as shown in Fig. 4(a), the phase diagram mapped to the two-dimensional plane is shown in Figure Fig. 4(b), where the colour shades represent the magnitude of ρ^*. It can be seen that in the phase diagram, there are three distinct regions of ρ^*, corresponding to the colours of yellow, blue and green, indicating that ρ^* under the influence of γ and α corresponds to three states when β and β^E are determined. So we artificially subdivide the original two types of equilibrium states into three states based on the final infection density. In the blue area, ρ^* is relatively small and converges to 0, it is called Disease-Free Equilibrium State. As for the green area, it is called General-Epidemic Equilibrium State because ρ^* is at the middle level, indicating the disease is severe. At the same time, the yellow area is referred to as Full-Domain Outbreak State, as ρ^* is so high that nearly all the individuals are at a high risk of being infected. The three states with marked colours are displayed in Fig. 5.

From the figure, the iso-infection density lines are found to converge to corresponding hyperbolas in the (α, γ) phase diagram, showing a very strong symmetry and indicating that both of the two parameters play a determinant role in the final

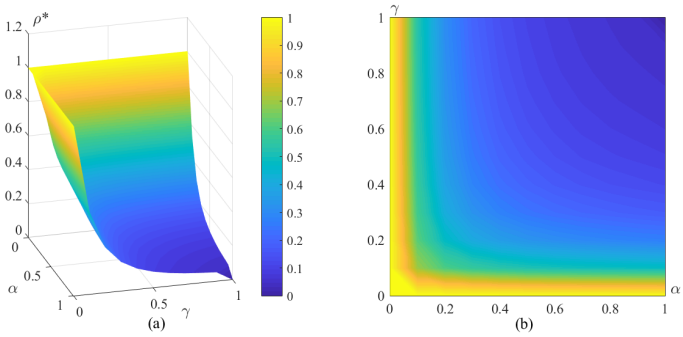

FIG. 4. (a) Three-dimensional variation diagram of $\rho^* - (\gamma, \alpha)$ and (b) two-dimensional planar phase diagram of it. Other parameters: $\beta = 0.01, \beta^E = 0.12, \delta = 0.001$.

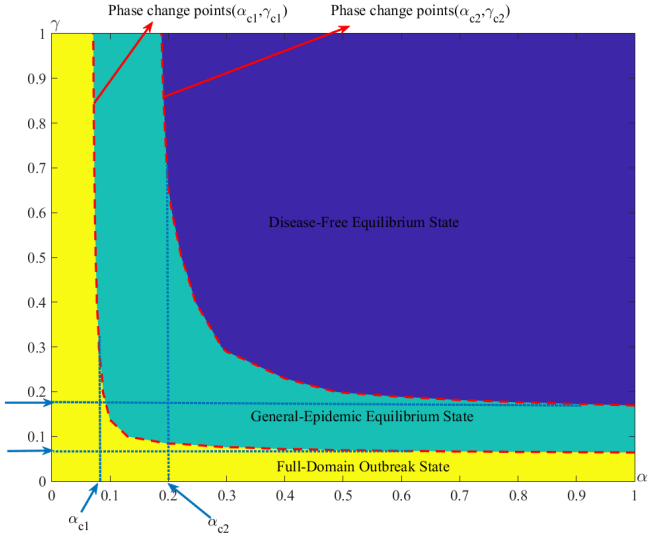

FIG. 5. The state phase diagram of $\rho^* - (\gamma, \alpha)$. The three colored areas represent the three states according to the final infection density. ***The yellow area has a very high infection density, nearly all nodes will have experienced at least one infection, and is recorded as the Full-Domain Outbreak State; the green area has a medium infection density and is recorded as the General-Epidemic Equilibrium State; the blue area has a very low infection density, most nodes may not have experienced infection, and the spread of the disease can be quickly suppressed by taking measures, so it is recorded as the Disease-Free Equilibrium State.***

infection size and they have a similar mechanism in the process of transmission. In the diagram, there are two hyperbolas giving two critical functions of (α, γ), denoted as $(\alpha_{c1}, \gamma_{c1})$, $(\alpha_{c2}, \gamma_{c2})$, which indicates the evolution of the three various states of the disease transmission process. And what catches our eyes is that a quite small value of either α or γ can lead the system to the Full-Domain Outbreak State, i.e., when the average latency days T_E or the average recovery days T_I are long enough, a widespread disease spread can easily occur, which is in line with the reality. Therefore, for diseases with small incubation days, such as common influenza, they are easier to control by medical means and usually do not spread on a large scale; while for viruses with long incubation periods, such as COVID-19, it is difficult to achieve disease clearance without implementing policies to intervene in the transmission process. ***This also gives us the insight that when a new epidemic reaches the General-Epidemic Equilibrium State or the Full-Domain Outbreak State, it is almost impossible to achieve a zero infection rate until an effective drug is developed. However, this does not mean that the epidemic should be completely ignored, and society needs to take more effective diagnostic measures to reduce the rate of misdiagnosis, and to provide timely, accurate and effective treatment to those infected. At the individual level, it is also recommended to take protective measures, such as insisting on wearing a mask when going out and always having some medication on hand.***

The experimental results are consistent with the theory of the model. The introduction of the expose rate α provides a source for the I-state nodes evolving from E state when a symptom appears, increasing the likelihood of being cured for the asymptomatic infected individuals. And the introduction of the recovery rate γ provides a destination for the I-state nodes, which is the only way for virus carriers to regain health. Also, the influence of α and γ is symmetric; either slow process can cause the recovery process of infected individuals to be blocked. In specific, a small value of α corresponds to the blocked exposing process, leading to the large amount of E-state nodes, while a small γ corresponds to the blocked recovery process, thus leading to I-state accumulation. Both the above effects can bring the expansion of the infection scale; that's why the system is in a Full-Domain Outbreak State when α or γ is small. Moreover, the symmetric effect of α and γ on the size of the infection is also reflected from the hyperbolic critical iso-infection density lines, which means, for a definite ρ^*, it exists a set of (α, γ) such that $c\alpha\gamma = \rho^*$ (c is a parameter depending on the system itself, the propagation rate, and the network structure, etc.). Therefore, the final infection size is proportional to the product of the expose rate and the recovery rate with a certain conditions.

3. The Effects of the Transmission Rate

In this section, we will study the effects of transmission rate β, β^E on the size of the transmission. In Fig. 6, the evolution of the spreading process over time was plotted by taking $\beta = 0.01, 0.03, 0.1, 0.3, 0.5$, with other parameters setting as $\beta^E = 1.2\beta$, the average latency day $T_E = 7$, the average recovery day $T_I = 21$, and the relative active node proportion $\delta = 0.001$. Generally speaking, proportions of nodes with I, E and V states are increasing over time, as shown in Fig. 6 (a) (b) and (c), respectively. Nevertheless, in Fig. 6(b), the 'shoulders' or 'peaks' phenomenon appears and gets more clear with increasing β. The reason is that, when β and β^E are large, a huge amount of people are getting infected to E state in a very short time, and when the time is shorter than the incubation period T_E, there is no enough time for the E-state nodes turning to I state, leading to the emergence of 'peaks' of E-state

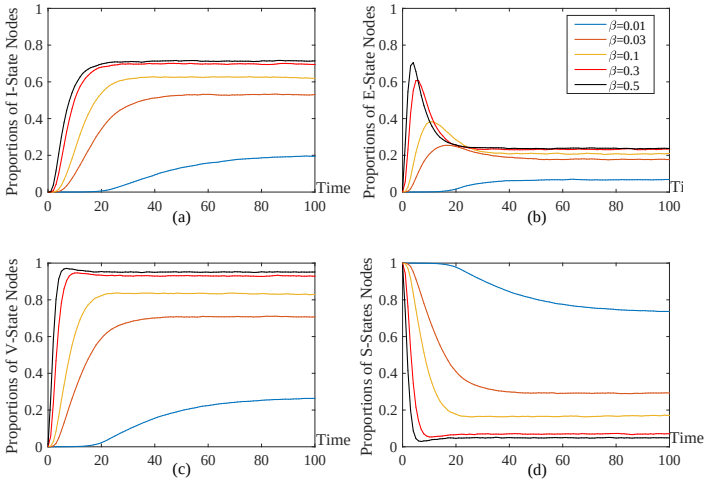

FIG. 6. Evolution curves of the proportions of each-state nodes with time for different β. Other parameter settings: $\beta_E = 1.2\beta, T_E = 7, T_I = 21, \delta = 0.001$.

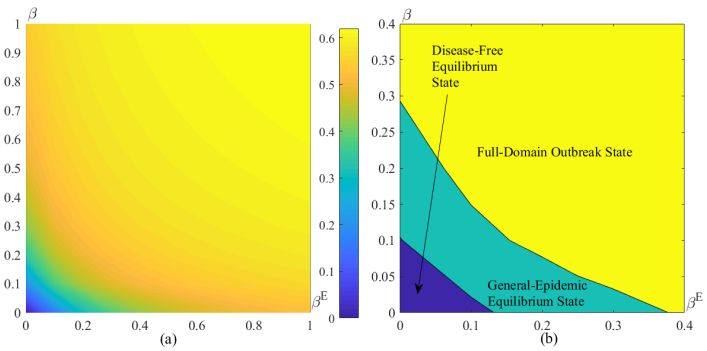

FIG. 7. (a) Two-dimensional planar phase diagram of $\rho^* - (\beta, \beta_E)$, in which three phases are recognized and marked with different colours. (b).Three-state transition diagram of $\rho^* - (\beta, \beta_E)$. Other parameters: $T_E = T_I = 7, \delta = 0.001$. ***The yellow area is the Full-Domain Outbreak State, the green area is the General-Epidemic Equilibrium State, the blue area is the Disease-Free Equilibrium State.***

nodes. As time steps increase to larger than T_E, the E state nodes will decrease because they can also turn to I state in a very short time. And finally, at a steady state, a balance is reached between the infection process and the expose process.

In the above simulation, it is assumed that there is a linear relationship between β and β^E. In a real system, however, the relationship between β and β^E are more complex. In Fig. 7, we investigate the combined effect of two propagation rates β and β_E, with $\beta \in [0,1]$, $\beta_E \in [0,1]$ in steps of 0.01. In the phase diagram, the order parameter is still ρ^*, with the remaining parameters setting as follows: the average latency day $T_E = 7$, the average recovery day $T_I = 7$, and the relative proportions of active nodes $\delta = 0.001$. From Fig. 7(a), there is also three states recognized roughly, which are distinguished by three colours, as shown in Fig. 7(b). It can be seen that with an increase of β, β^E, the system first transformed from the Disease-Free Equilibrium State (the domain marked in blue) to the General-Epidemic Equilibrium State (in green). And when β, β^E are increasing, ρ^* is getting larger, and most of the nodes in the system have been infected, thus there is a phase transition to the Full-Domain Outbreak State (the yellow area). Again, there are two critical curves of (β, β^E), in which the phase transition occurs to the systems.

Besides, we've found that the critical curves of (β, β^E) are related to (α, γ), as so the phase diagrams are plotted with a variety of $\frac{\alpha}{\gamma}$, the ratio of the expose rate to the recovery rate (also the ratio of the T_I to T_E), as well as two different values of δ, the relative proportion of active nodes, and the results shown in Fig. 8. When the ratio $\frac{\alpha}{\gamma}$ is small, the threshold of β_E is also smaller, which is manifested in the phase diagram as faster state transitions in the region closer to the β_E-coordinate side and reaching the Full-Domain Outbreak State first, otherwise, the state transitions in the region closer to the β_E-coordinate side is faster. This is because the smaller the ratio $\frac{\alpha}{\gamma}$ indicates that the recovery process is faster relative to the expose rate and the nodes linger in the E state, whereupon most S-state nodes are infected by E-state nodes, with the infection effect of β_E being enhanced and vice versa. Thus the threshold only depends on the values of β and β_E when the expose rate is equal to the recovery rate. At this level, the prominence of the expose rate and the recovery rate is prioritized over the transmission rate for the parameters that determine the threshold and the final size during the evolution of the disease. When formulating epidemic prevention policies, it is in essence the regulation of various parameters in the transmission process. ***Therefore, for infectious diseases such as COVID-19, which have both an incubation period and the potential to reinfect people, we can first consider how to regulate the incubation rate and recovery rate to control the development of the epidemic.***

IV. CONCLUSION

In this paper, we focus on the mobile crowds and the latent time of infectious diseases and deeply study the disease transmission behaviour caused by the mobile crowds travelling in different geographic spaces, so as to provide the theoretical basis for policy formulation and intervention in similar health events. We found that the existence of latent period makes the proportion of active nodes and the rate of virus transmission have a 'cumulative effect' on the number of patients, which will make the number of infected people increase in the process of 'peaks' or 'shoulders'. This has certain practical significance for the study of the transmission mechanism of latent infectious diseases. Specifically, to contain rapid outbreaks of infectious diseases, response measures should be taken before peaks are reached. More interestingly, we found that mobile crowds are not the determining factor that causes wide outbreaks without instant measures taken, because even few people moving among different spaces can quickly induce dis-

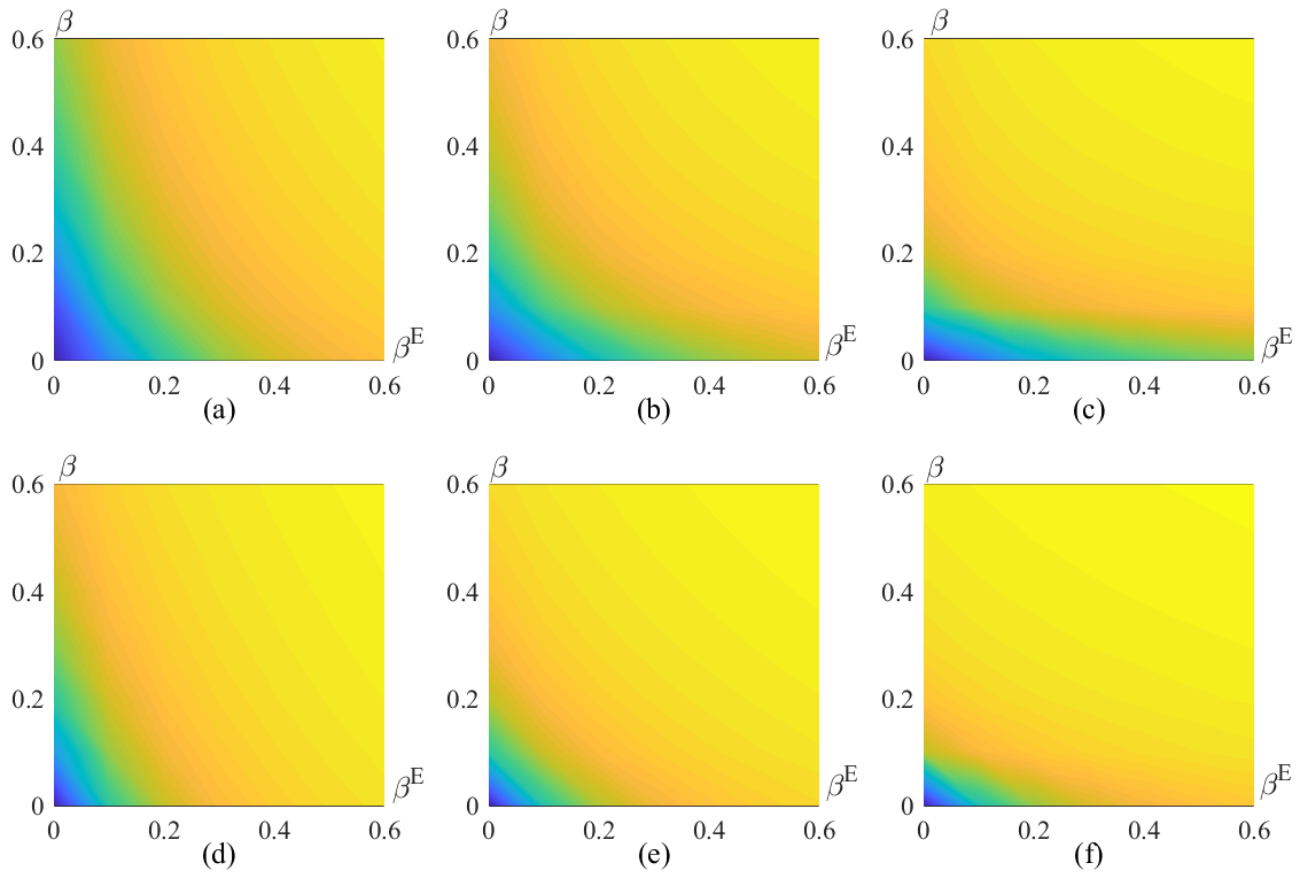

FIG. 8. Two-dimensional planar phase diagrams of $\rho^* - (\beta, \beta_E)$ for different parameters: (a)$\delta = 0.001, \frac{\alpha}{\gamma} = \frac{1}{2}$. (b)$\delta = 0.001, \frac{\alpha}{\gamma} = 1$. (c)$\delta = 0.001, \frac{\alpha}{\gamma} = 2$. (d)$\delta = 0.01, \frac{\alpha}{\gamma} = \frac{1}{2}$. (e)$\delta = 0.01, \frac{\alpha}{\gamma} = 1$. (f)$\delta = 0.001, \frac{\alpha}{\gamma} = 2$.

ease transmission. So for infectious diseases with an incubation period, to completely stop the widespread spread of the disease, it does prohibit the movement of the population, however, this has a great impact on social development and people's life, which is not a good strategy. Therefore, for diseases with lower mortality rates, it is recommended to adopt a liberalization policy and not restrict the movement of the population. ***Considering these two points together, when a new infectious disease emerges, it is more effective to take strong measures such as home isolation and disease screening before it reaches its peak; and when the disease has developed for a period of time or has reached its peak, it is no longer recommended to interrupt transmission by mass restriction of population movement.***

Furthermore, by traversing the relevant parameters in the model, we found that the combination of (β,β_E), (α,γ) can respectively cause mixed phase changes in the proportion of infected individuals, causing the system to shift among Disease-Free Equilibrium State, General-Epidemic Equilibrium State and Full-Domain Outbreak State. Most of the epidemic prevention policies are formulated by taking measures to change the values of these important parameters to regulate the transmission process. Therefore, the study of these phase change behaviours is more useful in choosing how to regulate the parameters to suppress a widespread outbreak.

We also find that in this model, the combination of expose rate α, and recovery rate γ has a higher priority on the influence of the final state of the system, and their ratio determines the propagation threshold of the system and the product determines the final evolution scale of the system. Therefore, when formulating relevant prevention strategies, the modulation of the two parameters should be considered first.

The model we construct here is applicable to the transmission behaviour of epidemics with latent period under different networks. However, the research in this paper is still mainly at the theoretical level, only on the model itself, and the applications based on the model require further discussion. Therefore, the future prospective work based on this paper is mainly: (1) Applications. Combined with the real-life transmission situation of the COVID-19 epidemic, the model is to be used in immunization strategies as well as resource allocation, and extra effort is also needed to optimize the model. (2) In-depth discussion of the transmission threshold. In this paper, the transmission threshold of the model was derived, however, due to the complexity of the question, it was not discussed in depth, and future research on this content will be

improved.

ACKNOWLEDGEMENT

This research is partially supported by the National Natural Science Foundation of China (Grant Nos. T2293771, 12171070, 71601030) and the Department of Science and Technology of Sichuan Province (Grant No. 2020YJ0266)

DATA AVAILABILITY STATEMENT

The data that support the findings of this study are available from the corresponding author upon reasonable request.

COMPETING INTEREST

The authors declare that they have no competing interests.

Appendix A: Notion of Main Symbol

Given that this paper contains a large number of symbols, the main symbols are listed in Table I for the convenience of the reader.

Appendix B: The Derivation Process of The Epidemic Threshold

Here we use the Jacobi matrix to find the epidemic threshold[9]. According to the deterministic difference equation about the V-state shown in Eq.(15), the vector form can be written as

$$\boldsymbol{P}(t+1) = g(\boldsymbol{P}(t)), \tag{B1}$$

and the elements of its Jacobi matrix are

$$[\nabla g(\mathbf{0})]_{i,j} = \begin{cases} \beta\eta(t) a^d_{ji} w^d_j(t) w^d_i(t) & j \neq i \\ 1-\gamma & j = i \end{cases}, \tag{B2}$$

where a^d_{ji} indicates whether nodes j and i are connected at the d_{th} layer, corresponding to the elements in the total adjacency matrix A_{Mul} of the multi-layer network.

The epidemic threshold, along with the propagation scale, is independent of the specific dynamical process, i.e., how exactly each time step propagates, but is determined by the internal characteristics of the system, so that the epidemic threshold can be directly derived from the steady-state situation. When the system reaches to the steady state, we have the layer probability vector $\boldsymbol{W}_{i-Act}(t) = \boldsymbol{W}_{i-Act}(t) = \boldsymbol{\pi}_{i-Act}$, so $w^d_j(t)$ and $w^d_i(t)$ both converge to π^d_j, π^d_i, then let $o_{ji}{}^* = \pi^d_j \pi^d_i$, whose meaning indicates the probability that nodes j and i are in the d_{th} level at the same time at steady state. Besides, we let the ratio of the number of E-state nodes to the number of I-state nodes at moment t be $1-\eta(t) : \eta(t)$, and according to Eq.(10), it's obviously at steady-state $\eta(t)$ coverges to a constant marked as η and it can be easily got that

$$\eta = \frac{\alpha}{\alpha+\gamma}. \tag{B3}$$

So at the steady state, Eq.(10) can be written as

$$[\nabla g(\mathbf{0})]_{i,j} = \begin{cases} \beta\eta a^d_{ji} o^{d*}_{ji} & j \neq i \\ 1-\gamma & j = i \end{cases} \tag{B4}$$

For analysis purposes, we introduce a matrix $\boldsymbol{B}$ defined as

$$\boldsymbol{B} = (b_{ij})_{\dim[A_{Mul}]} = \left(a_{ji}{}^d o_{ji}{}^{d*}\right)_{\dim[A_{Mul}]} \tag{B5}$$

where $\boldsymbol{A}_{Mul}$ means that the matrix $\boldsymbol{B}$, $\boldsymbol{A}_{Mul}$ has the same dimension.

And according to the symmetry of the adjacency matrix, Eq.(B2) can also be written as

$$\nabla g(\mathbf{0}) = \beta\eta\boldsymbol{B} + (1-\gamma)\boldsymbol{I}, \tag{B6}$$

where $\boldsymbol{I}$ is the unit matrix. Denote $\boldsymbol{S} = \nabla g(\mathbf{0})$ and S is the 'System Matrix' of the system, which reveals the disease evolution pattern when the virus is on the verge of extinction. $\boldsymbol{S}$ and $\boldsymbol{B}$ should have the same eigenvectors, so the correspondence of their eigenvalues is

$$\Lambda_{i,S} = \beta\eta\Lambda_{i,\boldsymbol{B}} + 1 - \gamma, \forall i, \tag{B7}$$

The condition that makes the system asymptotically stable at $\boldsymbol{P} = \mathbf{0}$ is that all the eigenvalues of the system matrix are less than 1, i.e., there is $\Lambda_{(i,S)} < 1, \forall i$. Let the maximum eigenvalue of the system matrix $\boldsymbol{S}$ be $\Lambda_{(max,S)}$ and the maximum eigenvalue of the corresponding matrix $\boldsymbol{B}$ be $\Lambda_{(max,B)}$, then we have

$$\Lambda_{\max,\boldsymbol{S}} = \beta\eta\Lambda_{\max,\boldsymbol{B}} + 1 - \gamma < 1, \tag{B8}$$

simplify to get

$$\frac{\beta}{\gamma} < \frac{1}{\eta\Lambda_{\max,B}}. \tag{B9}$$

So we have the epidemic threshold

$$\tau_c = \frac{1}{\eta\Lambda_{\max,\boldsymbol{B}}} = \left(1+\frac{\gamma}{\alpha}\right)\frac{1}{\Lambda_{\max,\boldsymbol{B}}}. \tag{B10}$$

when $\tau = \frac{\beta}{\gamma} < \tau_c$, the system is asymptotically stable and will converge to $\mathbf{0}$ when $\boldsymbol{P}$ is minimal and the disease will die out automatically, while when $\tau = \frac{\beta}{\gamma} > \tau_c$, the system is non-asymptotically stable and may lead to disease outbreak even when $\boldsymbol{P}$ is minimal. And according to the definition of γ, α, the epidemic threshold is also given by

$$\tau_C = \left(1+\frac{T_I}{T_E}\right)\frac{1}{\Lambda_{\max,B}}. \tag{B11}$$

where T_E is the average latency days and T_I is the average recovery days.

TABLE I. Notion of Main Symbol.

Notations	Names	Definitions
β	Transmission Rate(I-State nodes)	The probility of a susceptible node being infected by an infected node
β_E	Transmission Rate(I-State nodes)	The probility of a susceptible node being infected by an exposed node
α	Expose Rate	The probility of a exposed node being transformed to an infected node
γ	Recovery Rate	The probility of a infected node being transformed to a susceptible node
T_E	Average Latent Days	The average days of a node being exposed
T_I	Average Recovery Days	The average days of a node being infected
m		The number of static nodes on each layer
n		The number of the total active nodes
δ	The Relative Proportion of Active Nodes	$\delta = n/m$
i_{Act}		The specific active node i
$\boldsymbol{L}_{i-\text{ Act}}$	Inter-layer Transfer Matrix	To record the probabilities of i_{Act} transforming from one layer to another
$\boldsymbol{V}_{i-\text{ Act}}$	Layer State Vector	To determine whether i_{Act} is in layer d
$\boldsymbol{W}_{i-\text{ Act}}$	Layer Probability Vector	To record the probability that i_{Act} is in each layer
$\boldsymbol{\pi}_{i-\text{ Act}}$		To record the probability that i_{Act} is in each layer at steady state
$\boldsymbol{s}_i(t)$	Node State Vector	To record the transmission state of a node
$\boldsymbol{p}_i(t)$	Node Probability Vector	To denote the probability of the transmission state of node i
$\boldsymbol{S}^d(t)$		To store the states of all nodes in $d_t h$ layer
$\boldsymbol{G}^d(t)$		To store the number of neighbour nodes in each state for all nodes
$p_i^X(t)$		The probability of the node i being in state X at time t
$q_i(t)$		The probability of the node i being infected by its neighbor nodes at time t
ρ^*		The density of the nodes in state V under the steady state

[1] N. Dey, R. Mishra, S. J. Fong, K. C. Santosh, S. Tan, and R. G. Crespo, "Covid-19: Psychological and psychosocial impact, fear, and passion," Digital Government: Research and Practice **2**, 1–4 (2020).

[2] A. J. Kucharski, T. W. Russell, C. Diamond, Y. Liu, J. Edmunds, S. Funk, R. M. Eggo, and C.-W. G. Centre for Mathematical Modelling of Infectious Diseases, "Early dynamics of transmission and control of covid-19: a mathematical modelling study," Lancet Infect Disease **20**, 553–558 (2020).

[3] C. Buckee, A. Noor, and L. Sattenspiel, "Thinking clearly about social aspects of infectious disease transmission," Nature **595**, 205–213 (2021).

[4] S. Shukla, I. Tiwari, P. Sarin, and P. Parmananda, "Interventions and their efficacy in controlling the spread of an epidemic: A numerical study," Chaos: An Interdisciplinary Journal of Nonlinear Science **32**, 031102 (2022).

[5] N. Dong, X. Guan, J. Zhang, H. Zhou, J. Zhang, X. Liu, Y. Sun, P. Xu, Q. Li, and X. Hao, "Propagation dynamics and control policies of covid-19 pandemic at early stages: Implications on future resurgence response," Chaos: An Interdisciplinary Journal of Nonlinear Science **32**, 053102 (2022).

[6] Y. Cao, F. Jian, J. Wang, Y. Yu, W. Song, A. Yisimayi, J. Wang, R. An, X. Chen, N. Zhang, Y. Wang, P. Wang, L. Zhao, H. Sun, L. Yu, S. Yang, X. Niu, T. Xiao, Q. Gu, F. Shao, X. Hao, Y. Xu, R. Jin, Z. Shen, Y. Wang, and X. S. Xie, "Imprinted sars-cov-2 humoral immunity induces convergent omicron rbd evolution," Nature **614**, 521–529 (2023).

[7] P. Van Mieghem, J. Omic, and R. Kooij, "Virus spread in networks," IEEE/ACM Transactions on Networking **17**, 1–14 (2009).

[8] R. Pastor-Satorras, C. Castellano, P. Van Mieghem, and A. Vespignani, "Epidemic processes in complex networks," Reviews of Modern Physics **87**, 925–979 (2015).

[9] D. Chakrabarti, Y. Wang, C. Wang, J. Leskovec, and C. Faloutsos, "Epidemic thresholds in real networks," ACM Transactions on Information and System Security **10**, 1–26 (2008).

[10] R. Pastor-Satorras and A. Vespignani, "Epidemic spreading in scale-free networks," Physical Review Letters **86**, 3200–3 (2001).

[11] M. R. Sanatkar, W. N. White, B. Natarajan, C. M. Scoglio, and K. A. Garrett, "Epidemic threshold of an sis model in dynamic switching networks," IEEE Transactions on Systems, Man, and Cybernetics: Systems **46**, 345–355 (2016).

[12] M. Kiamari, G. Ramachandran, Q. Nguyen, E. Pereira, J. Holm, and B. Krishnamachari, "Covid-19 risk estimation using a time-varying sir-model," in *Proceedings of the 1st ACM SIGSPATIAL International Workshop on Modeling and Understanding the Spread of COVID-19*, COVID-19 (Association for Computing Machinery, New York, NY, USA, 2020) p. 36–42.

[13] M. Cai, G. Em Karniadakis, and C. Li, "Fractional SEIR model and data-driven predictions of COVID-19 dynamics of Omicron variant," Chaos: An Interdisciplinary Journal of Nonlinear Science **32** (2022).

[14] Y. Ding, Y. Fu, and Y. Kang, "Stochastic analysis of COVID-19 by a SEIR model with Lévy noise," Chaos: An Interdisciplinary Journal of Nonlinear Science **31** (2021).

[15] A. Eilersen, B. F. Nielsen, and K. Sneppen, "Tradeoff between speed and reproductive number in pathogen evolution," Physical Review Research **5**, 023003 (2023).

[16] L. Gostiaux, W. J. T. Bos, and J.-P. Bertoglio, "Periodic epidemic outbursts explained by local saturation of clusters," Physical Review E **107**, L012201 (2023).

[17] J. S. Weitz, S. W. Park, C. Eksin, and J. Dushoff, "Awareness-driven behavior changes can shift the shape of epidemics away from peaks and toward plateaus, shoulders, and oscillations," Proceedings of the National Academy of Sciences of the United States of America **117**, 32764–32771 (2020).

[18] I. A. Perez, M. A. Di Muro, C. E. La Rocca, and L. A. Braunstein, "Disease spreading with social distancing: A prevention strategy in disordered multiplex networks," Physical Review E **102**, 022310 (2020).

[19] J. Hindes, M. Assaf, and I. B. Schwartz, "Outbreak size distribution in stochastic epidemic models," Physical Review Letters **128**, 078301 (2022).

[20] G. St-Onge, H. Sun, A. Allard, L. Hébert-Dufresne, and G. Bianconi, "Universal nonlinear infection kernel from heterogeneous exposure on higher-order networks," Physical Review Letters **127**, 158301 (2021).

[21] L. Matrajt, J. Eaton, T. Leung, and E. R. Brown, "Vaccine optimization for covid-19: Who to vaccinate first?" Science Advances **7**, eabf1374 (2021).

[22] S. Han, J. Cai, J. Yang, J. Zhang, Q. Wu, W. Zheng, H. Shi, M. Ajelli, X. H. Zhou, and H. Yu, "Time-varying optimization of covid-19 vaccine prioritization in the context of limited vaccination capacity," Nature Communication **12**, 4673 (2021).

[23] J. Li, C. Yang, X. Ma, Y. Gao, C. Fu, and H. Yang, "Suppressing epidemic spreading by optimizing the allocation of resources between prevention and treatment," Chaos: An Interdisciplinary Journal of Nonlinear Science **29**, 113108 (2019).

[24] L. Bottcher, O. Woolley-Meza, E. Goles, D. Helbing, and H. J. Herrmann, "Connectivity disruption sparks explosive epidemic spreading," Physical Review E **93**, 042315 (2016).

[25] S. Boccaletti, G. Bianconi, R. Criado, C. I. Del Genio, J. Gomez-Gardenes,

M. Romance, I. Sendina-Nadal, Z. Wang, and M. Zanin, "The structure and dynamics of multilayer networks," Physics Reports **544**, 1–122 (2014).
[26]M. Kivelä, A. Arenas, M. Barthelemy, J. P. Gleeson, Y. Moreno, and M. A. Porter, "Multilayer networks," Journal of Complex Networks **2**, 203–271 (2014).
[27]G. Bianconi, *Multilayer Networks: Structure and Function* (Oxford University Press, 2018).
[28]P. Bródka, J. Jankowski, and R. Michalski, "Sequential seeding in multilayer networks," Chaos: An Interdisciplinary Journal of Nonlinear Science **31**, 033130 (2021).
[29]F. Velásquez-Rojas, P. C. Ventura, C. Connaughton, Y. Moreno, F. A. Rodrigues, and F. Vazquez, "Disease and information spreading at different speeds in multiplex networks," Physical Review E **102**, 022312 (2020).
[30]L. Zhu, W. Liu, and Z. Zhang, "Interplay between epidemic and information spreading on multiplex networks," Mathematics and Computers in Simulation **188**, 268–279 (2021).
[31]A. Tejedor, A. Longjas, E. Foufoula-Georgiou, T. T. Georgiou, and Y. Moreno, "Diffusion dynamics and optimal coupling in multiplex networks with directed layers," Physical Review X **8**.
[32]C. Li, Z. Yuan, and X. Li, "Epidemic threshold in temporal multiplex networks with individual layer preference," IEEE Transactions on Network Science and Engineering **PP**, 1–1 (2021).
[33]D. Ku, C. Yeon, S. Lee, K. Lee, K. Hwang, Y. C. Li, and S. C. Wong, "Safe traveling in public transport amid covid-19," Science Advances **7**, eabg3691 (2021).
[34]I. Mishkovski, M. Mirchev, S. Šćepanović, and L. Kocarev, "Interplay between spreading and random walk processes in multiplex networks," IEEE Transactions on Circuits and Systems I: Regular Papers **PP**, 1–11 (2017).
[35]S. Gómez, A. Arenas, J. Borge-Holthoefer, S. Meloni, and Y. Moreno, "Discrete-time markov chain approach to contact-based disease spreading in complex networks," EPL (Europhysics Letters) **89** (2010).
[36]J. S. Jia, X. Lu, Y. Yuan, G. Xu, J. Jia, and N. A. Christakis, "Population flow drives spatio-temporal distribution of covid-19 in china," Nature **582**, 389–394 (2020).

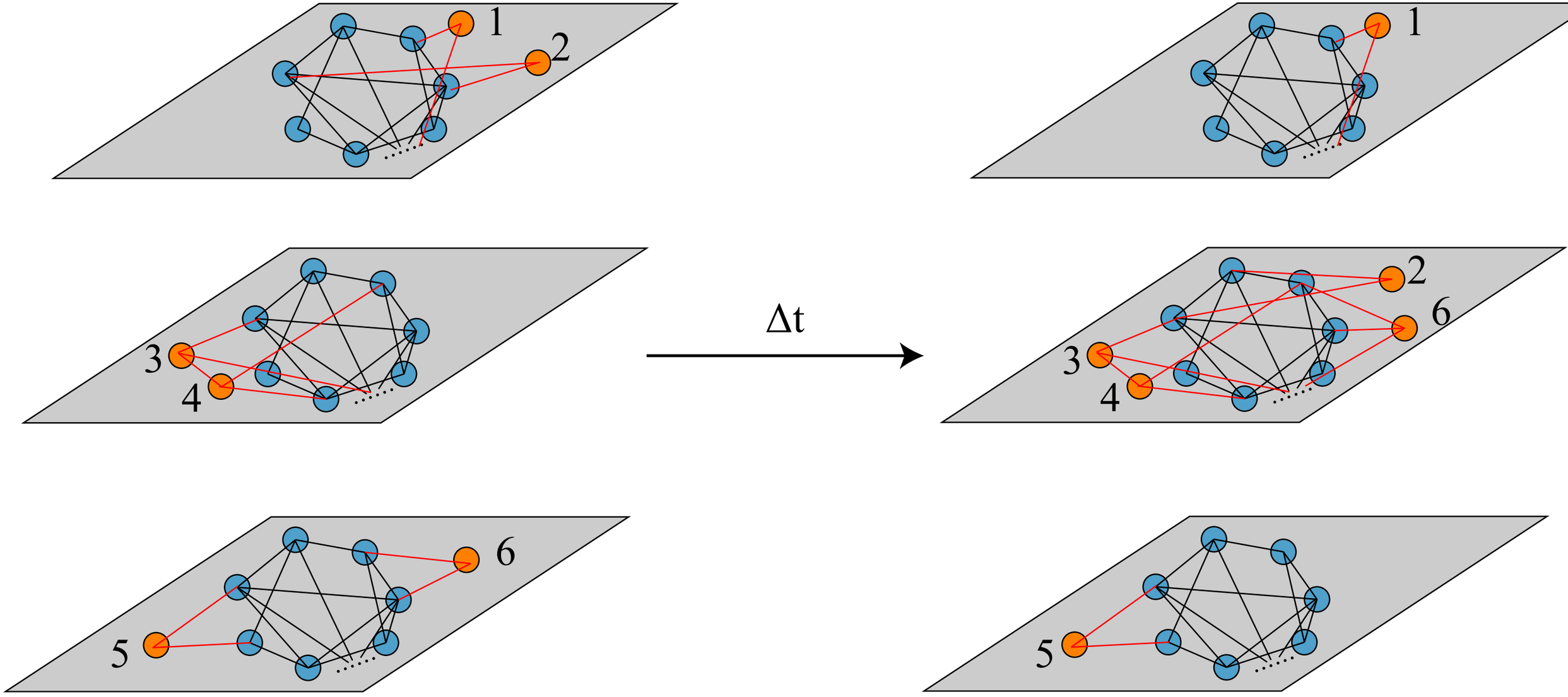
1
2
3
4
5
6
Δt

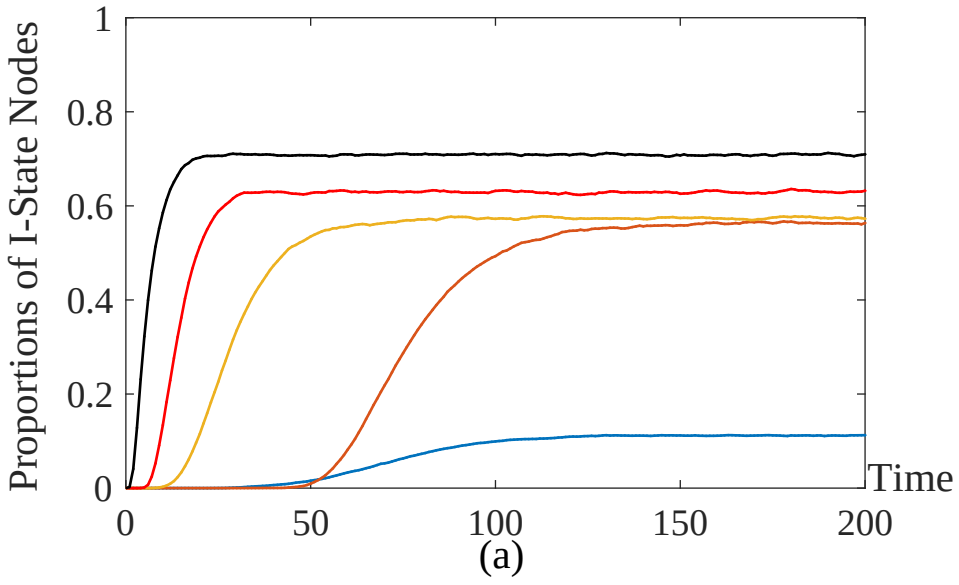
Proportions of I-State Nodes
Time
0
0.2
0.4
0.6
0.8
1
0
50
100
150
200

(a)

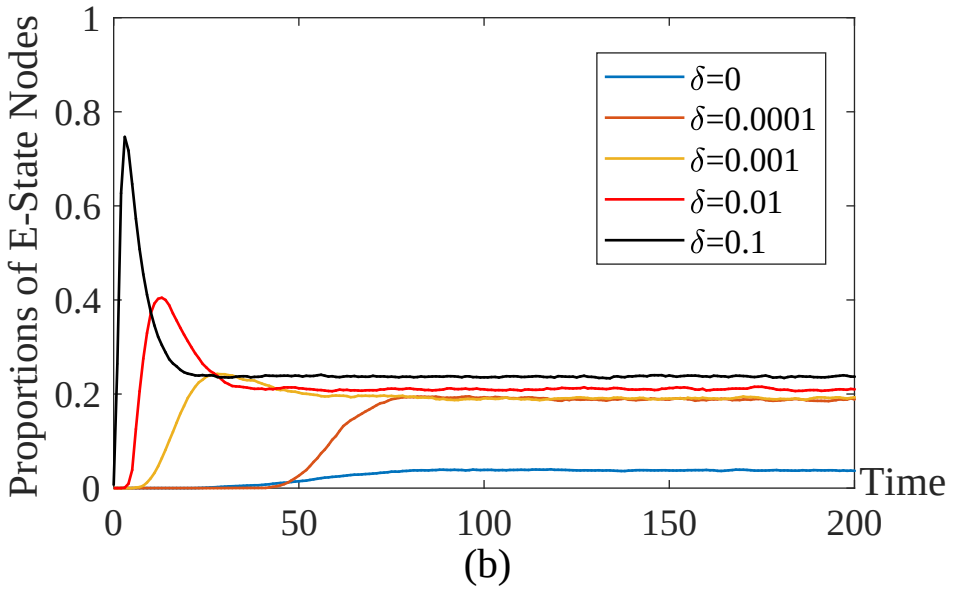
Proportions of E-State Nodes
Time
δ=0
δ=0.0001
δ=0.001
δ=0.01
δ=0.1
0
0.2
0.4
0.6
0.8
1
0
50
100
150
200

(b)

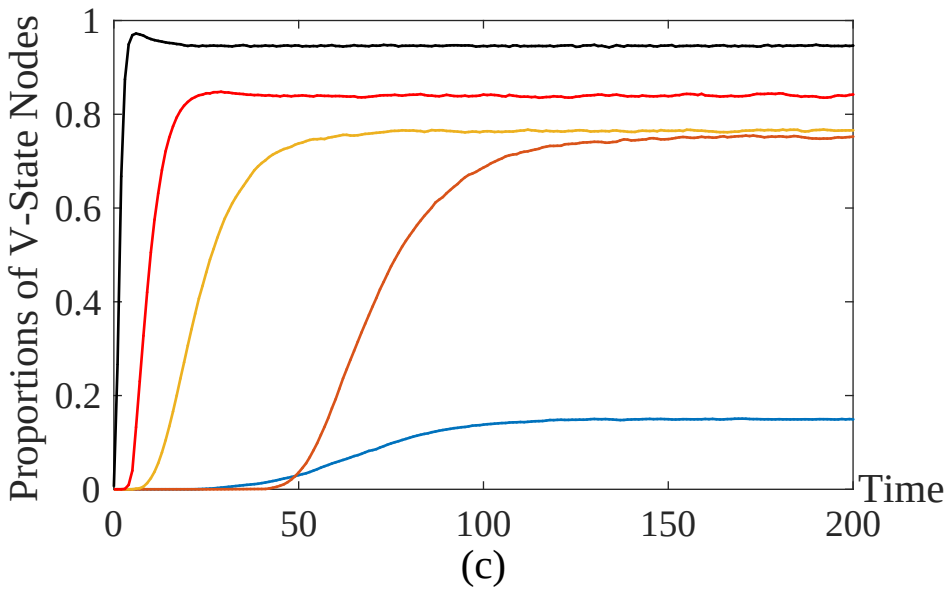
Proportions of V-State Nodes
Time
0
0.2
0.4
0.6
0.8
1
0
50
100
150
200

(c)

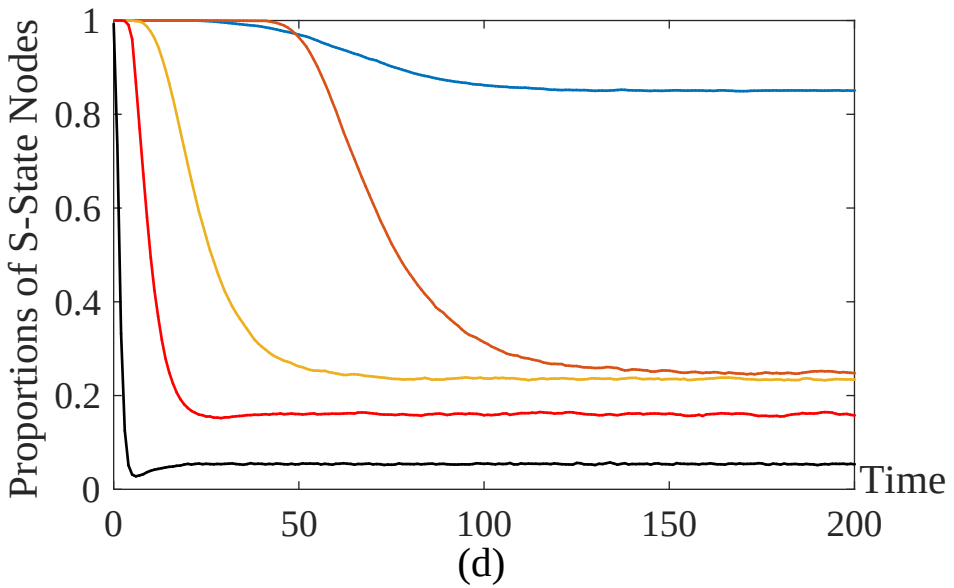
Proportions of S-State Nodes
Time
0
0.2
0.4
0.6
0.8
1
0
50
100
150
200

(d)

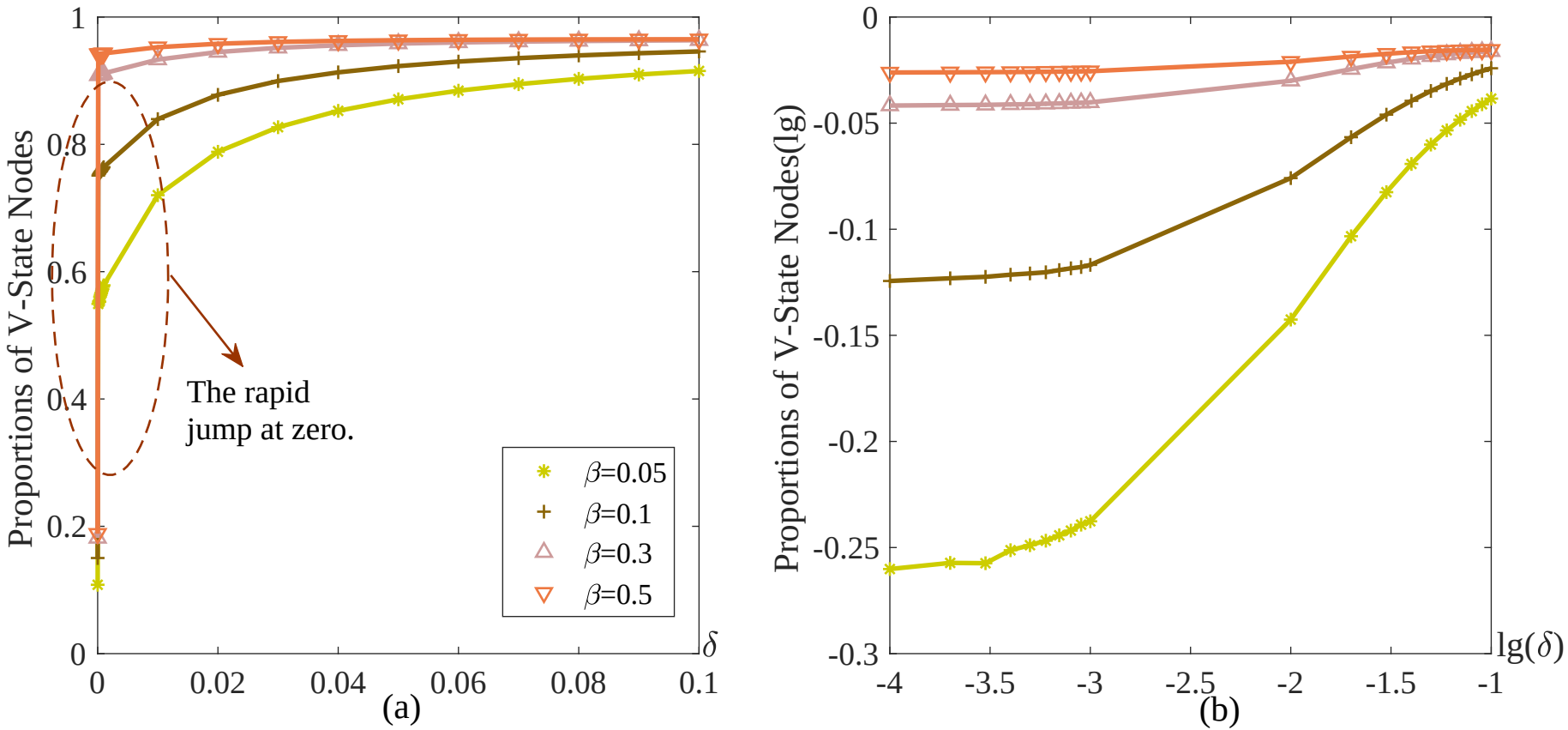
Proportions of V-State Nodes
1
0.8
0.6
0.4
0.2
0
0
0.02
0.04
0.06
0.08
0.1
δ
The rapid
jump at zero.
β=0.05
β=0.1
β=0.3
β=0.5
(a)
Proportions of V-State Nodes(lg)
0
-0.05
-0.1
-0.15
-0.2
-0.25
-0.3
-4
-3.5
-3
-2.5
-2
-1.5
-1
lg(δ)
(b)

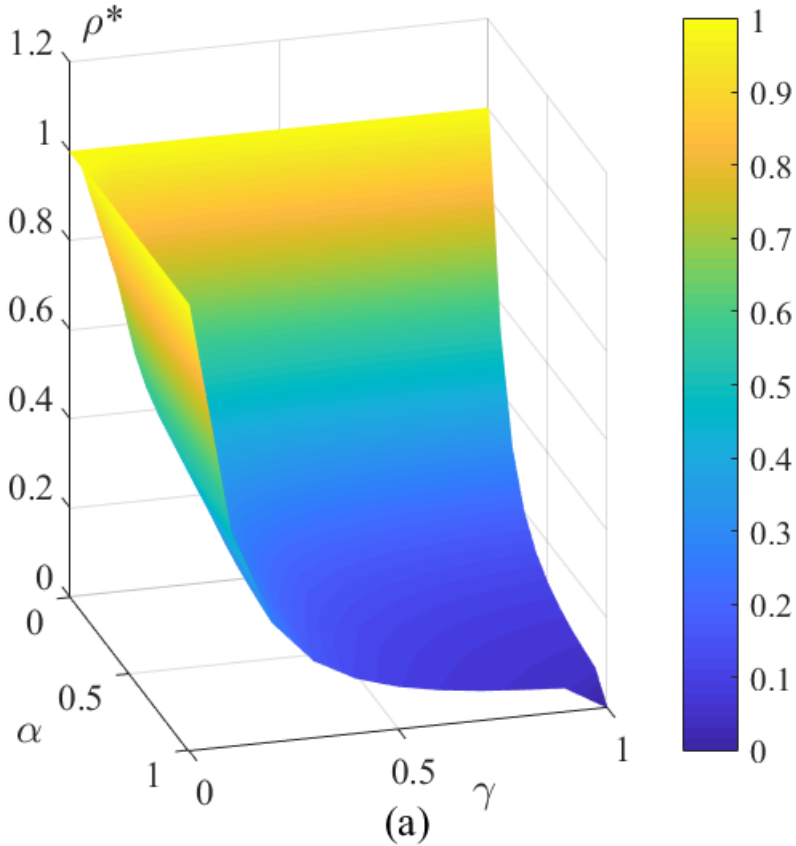
ρ*
1.2
1
0.8
0.6
0.4
0.2
0
0
0.5
α
1
0
0.5
γ
1
1
0.9
0.8
0.7
0.6
0.5
0.4
0.3
0.2
0.1
0

(a)

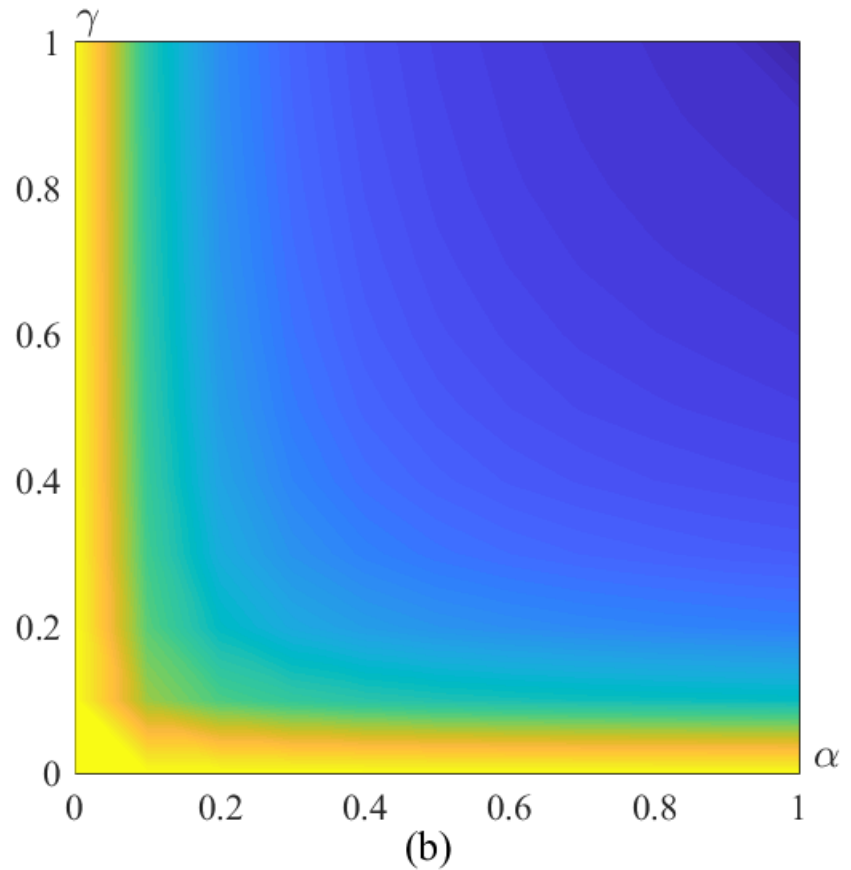
γ
1
0.8
0.6
0.4
0.2
0
0
0.2
0.4
0.6
0.8
1
α

(b)

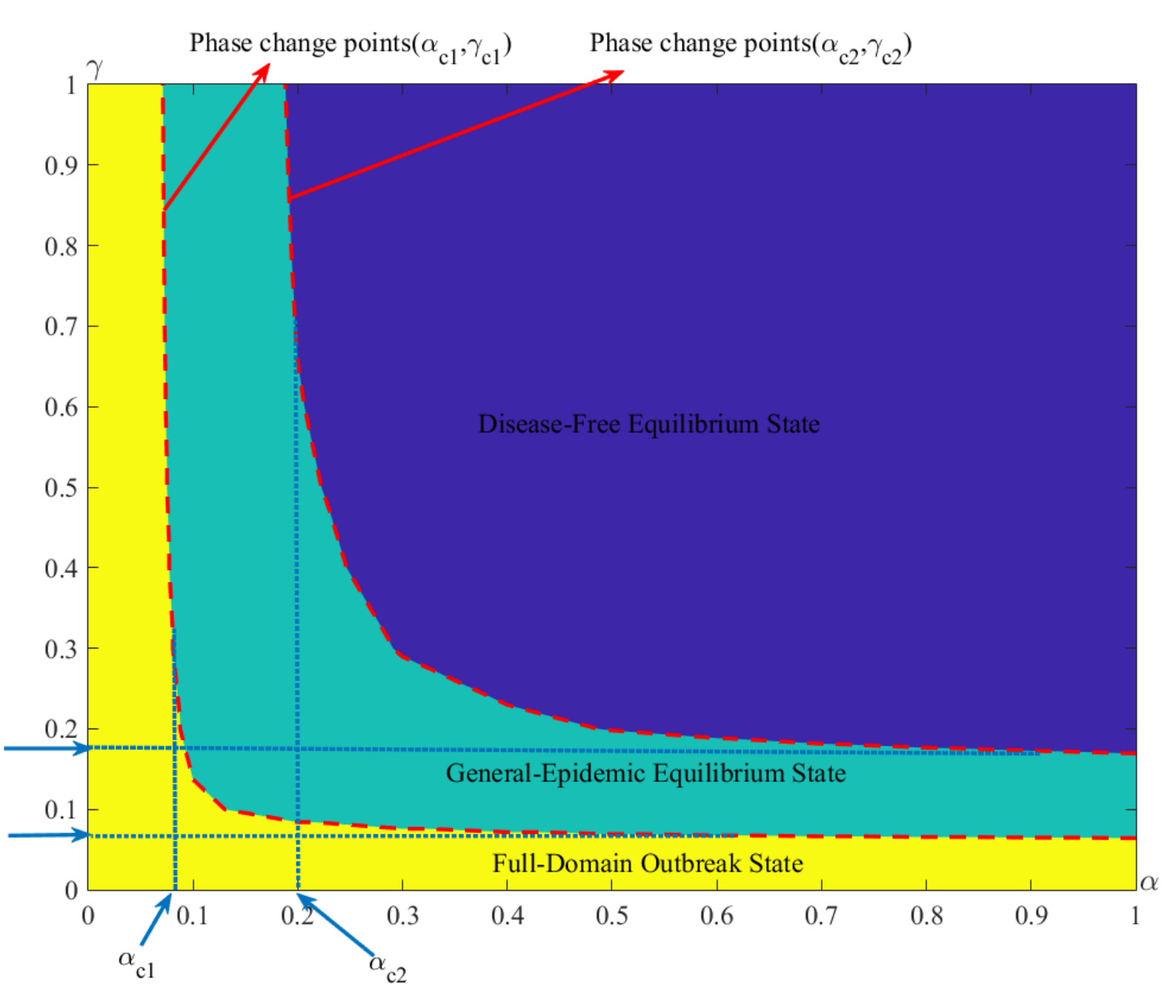
Phase change points(α_{c1},γ_{c1})
Phase change points(α_{c2},γ_{c2})
γ
α
Disease-Free Equilibrium State
General-Epidemic Equilibrium State
Full-Domain Outbreak State
α_{c1}
α_{c2}
0
0.1
0.2
0.3
0.4
0.5
0.6
0.7
0.8
0.9
1

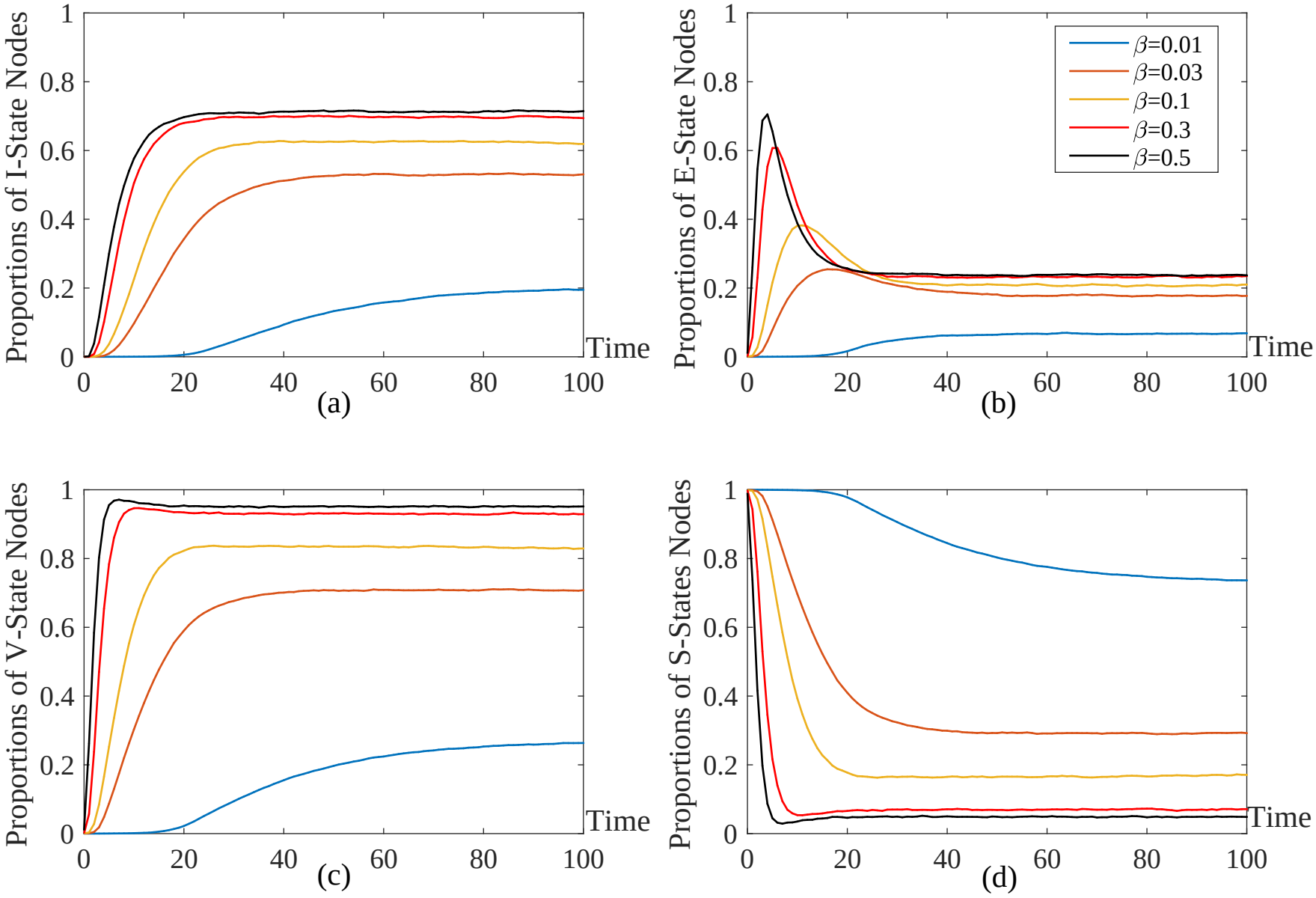
Proportions of I-State Nodes
Time
(a)
Proportions of E-State Nodes
Time
(b)
β=0.01
β=0.03
β=0.1
β=0.3
β=0.5
Proportions of V-State Nodes
Time
(c)
Proportions of S-States Nodes
Time
(d)

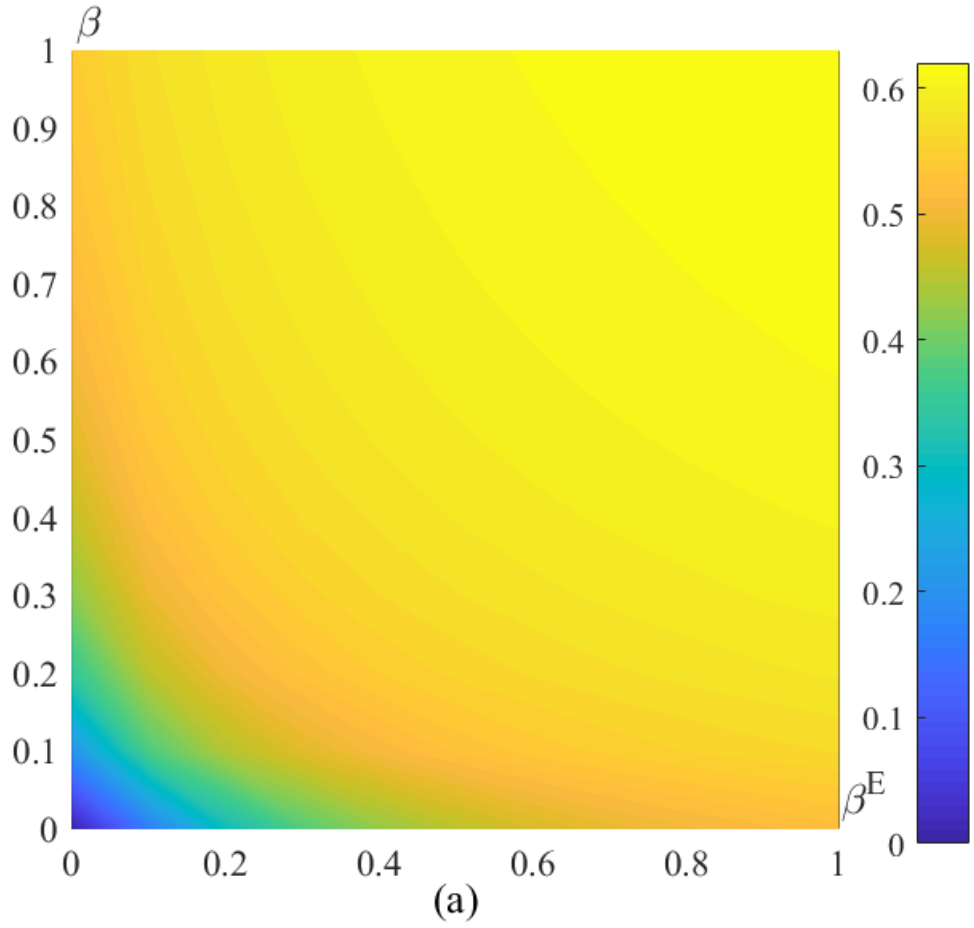
β
1
0.9
0.8
0.7
0.6
0.5
0.4
0.3
0.2
0.1
0
0
0.2
0.4
0.6
0.8
1
β^E
0.6
0.5
0.4
0.3
0.2
0.1
0
(a)

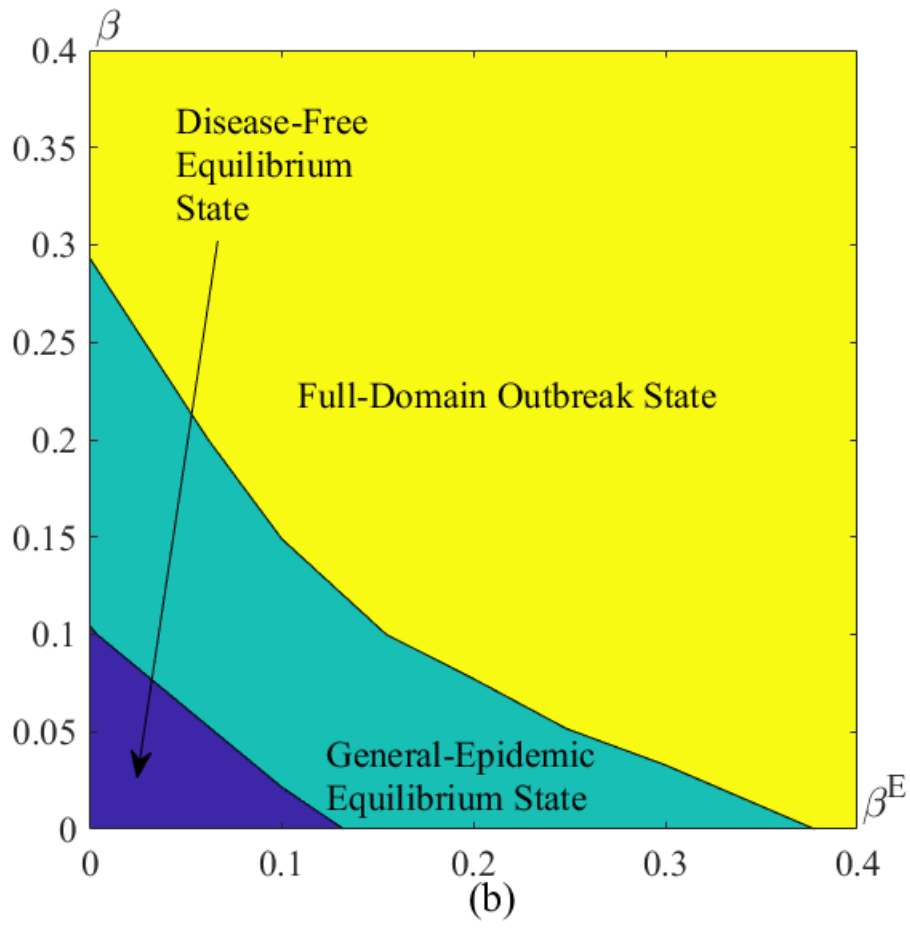
β
0.4
0.35
0.3
0.25
0.2
0.15
0.1
0.05
0
Disease-Free
Equilibrium
State
Full-Domain Outbreak State
General-Epidemic
Equilibrium State
0
0.1
0.2
0.3
0.4
β^E
(b)

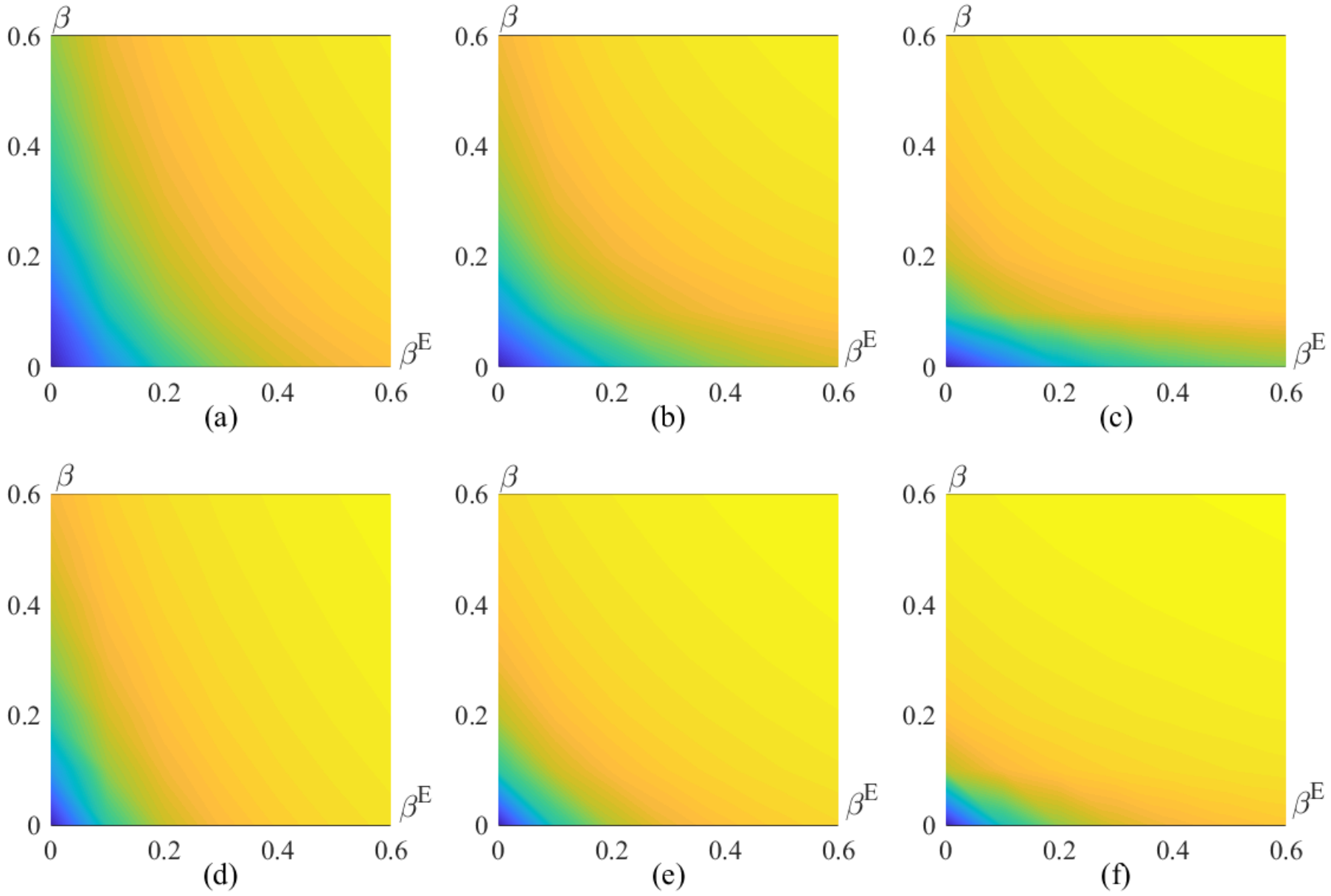
β
0.6
0.4
0.2
0
0
0.2
0.4
0.6
β^E
(a)
(b)
(c)
(d)
(e)
(f)